Chapter 12

ELECTROMECHANICS OF INCOMPRESSIBLE, INVISCID FLUIDS

12.0 INTRODUCTION

We are all familiar with the distinctions between the three pure states of matter: solids, liquids, and gases. A solid body possesses a definite shape and size that is retained unless the body is acted on by outside forces. A given mass of liquid possesses a definite size (volume) but conforms in shape to its container. A particular mass of gas possesses neither definite size (volume) nor shape because it will deform to fill completely whatever vessel it occupies.

Liquids and gases are grouped together and called fluids when their dynamic behavior is to be studied. The essential difference between a solid and a fluid is that the force necessary to deform a solid is a function of the deformation (strain), whereas in a fluid the force necessary to produce a deformation is a function of the *rate* of deformation (strain rate) and a hydrostatic pressure. A fluid left to itself in a force-free environment will relax to a state that has no internal stresses except an isotropic (hydrostatic) pressure balanced by the surface forces exerted by the container or by surface tension.

Although because of some similarities liquids and gases are classified together as fluids, they also exhibit striking differences. Moderate changes in temperature and pressure cause very small fractional changes in the density of a liquid but the corresponding changes in a gas are quite large.

All real fluids exhibit internal friction that is described mathematically by the property called *viscosity*. The effects of viscosity can be large or small, depending on the physical situation being studied. It is standard practice for an electrical engineer to represent a real coil of wire mathematically by an

ideal, lossless circuit element called inductance. Similarly, the fluid dynamicist often uses an idealization of a fluid in which viscosity is neglected. Such an idealization is called an *inviscid* fluid.

In most electromechanical systems involving fluids the principal effects of viscosity result from the contact between the fluid and a solid boundary. As in most continuum problems, the effect of the boundary becomes less pronounced at greater distances from the boundary. Thus, when the behavior of a fluid is desired far from a boundary, an inviscid model is often adequate. How a distance that is adequate for the neglect of viscosity is determined is a rather complex subject and depends quite naturally on the system to be analyzed and the accuracy desired. Much experimental and theoretical data are available to answer this question.* We address ourselves to a few simple cases in which viscosity is important in Chapter 14.

Our purpose in this book is to present models and do analyses of systems in which electromechanical interactions are important. This means essentially that for coupling with a fluid the electromechanical forces must dominate the viscous forces. It is fortuitous that many situations exist in which this occurs, notably magnetohydrodynamic pumps and generators and plasma accelerators.† Consequently, our use of an inviscid fluid model is realistic with respect to the dominant electromagnetic forces and viscous effects can be added later as perturbations.

When a fluid flows past a solid boundary, the fluid friction makes the fluid particles that are in contact with the boundary remain at rest with respect to the boundary. This makes the flow of fluid parallel to the boundary vary with distance from the boundary and introduces a shear rate into the flow. At low velocities each fluid particle flows along a smooth path (a streamline), and the flow is said to be *laminar*. At high velocities the shearing effect of the boundary makes the flow unstable and each fluid particle has a significant random motion in addition to its average motion in the direction of flow. This flow regime is said to be *turbulent*. When a flow becomes turbulent, its internal friction (viscous) losses increase. In spite of this, we can often represent a fluid in turbulent flow in terms of a steady flow at the average velocity and obtain a good model for electromechanical interactions.

Compressibility is a property of a fluid that describes the fact that when the hydrostatic pressure on the fluid is increased the density increases. Every fluid exhibits this property to some extent. Liquids are only slightly compressible, whereas gases are highly compressible. Compressibility to fluids is

* H. Schlichting, *Boundary Layer Theory*, 4th ed., McGraw-Hill, New York, 1960, pp. 1–41.

† These situations are illustrated graphically in the film entitled "Magnetohydrodynamics" produced for the National Committee on Fluid Mechanics Films by Education Development Center, Newton, Mass.

what elastic modulus is to elastic solids. Thus we expect a compressible fluid to transmit longitudinal (sound) waves just as an elastic solid does. When we are interested in the flow of a liquid, the compressibility can often be neglected. This is analogous to the treatment of the gross motion of an elastic solid as the motion of a rigid body. Even though a gas is highly compressible, we can sometimes treat gas flow by using an incompressible fluid model, especially at very low flow velocities. In other cases the compressibility of a gas will have a marked effect on the flow, and we must account for it in our mathematical model.

Our interest here is in electromechanical interactions; in each case we select the simplest mathematical model that illustrates the physical phenomena of interest in a realistic way. Thus in many cases we use a simple fluid model that adequately illustrates the electromechanical interactions but ignores some fluid-mechanical phenomena. The inclusion of such phenomena is beyond the scope of this book. For further information on these topics the reader can consult a good treatise on fluid mechanics.* In this chapter we investigate various phenomena that result from electromechanical interactions with incompressible, inviscid fluids. In Chapter 13 we treat compressible inviscid fluids and in Chapter 14 introduce viscosity.

12.1 INVISCID, INCOMPRESSIBLE FLUIDS

An incompressible inviscid fluid model lends itself to simple mathematical analysis and to an understanding of many fluid-mechanical phenomena. Moreover, it provides considerable insight into the fundamental interactions of magnetohydrodynamics (MHD) and often gives an accurate description of MHD interactions with liquid conductors such as liquid metals.

In what follows we first introduce the equations of motion for an incompressible inviscid fluid and then consider some simple, fluid-mechanical examples. Finally, we investigate the important electromechanical interactions appropriate for study with this model.

12.1.1 The Substantial Derivative

In the study of fluid mechanics we are concerned with describing the fluid motion and relating it to the applied forces and boundary conditions. Most often the desired information consists of determining a flow pattern in a region of space at a given instant of time. Because of this desired result, fluid dynamicists have focused their attention on fluid variables at a given position in relation to a fixed reference frame. Since the fluid is moving past this point, different material elements occupy the point at different instants in time. This

* See, for example, Schlichting, *op. cit.*

method of representing fluid properties (such as velocity) in terms of a fixed point in space is called an Eulerian or field description. An alternative method, called the Lagrangian description, gives the velocity and other properties of the individual particles.

The best-known example of the use of the Lagrangian description is in particle dynamics (or the rigid-body mechanics of Chapter 2) in which it is conventional to ascribe to each particle (or mechanical node) a velocity $\mathbf{v}$ which is a function of the initial position (a, b, c) of the particle and of time t. Thus $\mathbf{v}(a, b, c, t)$ describes the velocity of a particular particle. This same method is carried over into continuum mechanics by describing the velocity $\mathbf{v}(a, b, c, t)$ of the grain of matter at position a, b, c at $t = 0$. This Lagrangian description was used in Chapter 11, in which the displacement of a grain of elastic material was written as a function of the unstrained (initial) position.

For electrical engineering students the best-known example of the use of an Eulerian description is in electromagnetic field theory. We usually describe the electromagnetic field and source quantities as functions of space and time. Thus for a cartesian coordinate system (x_1, x_2, x_3) we give the electric field intensity as $\mathbf{E}(x_1, x_2, x_3, t)$. This prescribes the field intensity at the point (x_1, x_2, x_3) at any instant of time t. Using the Eulerian description, we can describe a velocity field $\mathbf{v}(x_1, x_2, x_3, t)$ that ascribes a velocity to a position in space rather than to a particular grain of matter. At the point (x_1', x_2', x_3') the velocity $\mathbf{v}(x_1', x_2', x_3', t')$ specifies the velocity of that grain of matter that occupies the point (x_1', x_2', x_3') at the instant of time t'. If at a later time t'' this grain of matter is at point (x_1'', x_2'', x_3''), its velocity will be $\mathbf{v}(x_1'', x_2'', x_3'', t'')$. The Eulerian system is normally used in the study of fluid mechanics and is also used here.*

Later in this chapter we shall need the time derivative of an Eulerian function as experienced by a particular grain of matter. The acceleration of a grain of matter is such a derivative and we shall need it to write Newton's second law.

Consider a system of moving matter with an Eulerian or field description of the velocity, $\mathbf{v}(x_1, x_2, x_3, t)$ and of the quantity $f(x_1, x_2, x_3, t)$. It is necessary to find the time rate of change of f experienced by a grain of matter. Consider the grain of matter that occupies position (x_1, x_2, x_3) at time t and has velocity $\mathbf{v}(x_1, x_2, x_3, t)$ with components v_1, v_2, and v_3. At time $(t + \Delta t)$ the grain will occupy a new position, given to first order in (Δt) by $(x_1 + v_1 \Delta t, x_2 + v_2 \Delta t, x_3 + v_3 \Delta t)$. Thus in the interval (Δt) the grain has experienced a change in f of

$$\Delta f = f(x_1 + v_1 \Delta t, x_2 + v_2 \Delta t, x_3 + v_3 \Delta t, t + \Delta t) - f(x_1, x_2, x_3, t) \quad (12.1.1)$$

* For a more thorough discussion of these alternative representations, see, for example, H. Lamb, *Hydrodynamics*, 6th ed., Dover, New York, 1945, Chapter I, Articles, 4 to 9, 13, and 14.

The first term in this expression is expanded in a Taylor series about the point (x_1, x_2, x_3, t) and second- and higher order terms in Δt are discarded to obtain

$$\Delta f = \frac{\partial f}{\partial t}\Delta t + \frac{\partial f}{\partial x_1} v_1 \Delta t + \frac{\partial f}{\partial x_2} v_2 \Delta t + \frac{\partial f}{\partial x_3} v_3 \Delta t. \tag{12.1.2}$$

The desired time rate of change is defined as

$$\frac{Df}{Dt} = \lim_{\Delta t \to 0} \frac{\Delta f}{\Delta t}. \tag{12.1.3}$$

Substitution of (12.1.2) into (12.1.3) yields

$$\frac{Df}{Dt} = \frac{\partial f}{\partial t} + v_1 \frac{\partial f}{\partial x_1} + v_2 \frac{\partial f}{\partial x_2} + v_3 \frac{\partial f}{\partial x_3}, \tag{12.1.4}$$

which is written in the compact form

$$\frac{Df}{Dt} = \frac{\partial f}{\partial t} + (\mathbf{v} \cdot \nabla) f. \tag{12.1.5}$$

The function f may be considered to be one component of a cartesian vector $\mathbf{f}$. Equation 12.1.5 holds for each component of the vector; consequently, the time rate of change of a vector field quantity $\mathbf{f}(x_1, x_2, x_3, t)$ experienced by a grain of matter is given by

$$\frac{D\mathbf{f}}{Dt} = \frac{\partial \mathbf{f}}{\partial t} + (\mathbf{v} \cdot \nabla)\mathbf{f}. \tag{12.1.6}$$

This derivative is variously called the Stokes, total, particle, material, substantial, or convective derivative.

The interpretation of the physical meaning of (12.1.5) or (12.1.6) is quite simple. It merely states that an observer moving with the velocity $\mathbf{v}$, relative to the coordinate system (x_1, x_2, x_3) in which the quantity $f(x_1, x_2, x_3, t)$ is defined, will detect a time rate of change of f made up of two parts: $(\partial f/\partial t)$ is the rate of change of f at a fixed point and $(\mathbf{v} \cdot \nabla) f$ is the change in f that results from the motion of the observer through a fixed (in time) distribution of f. In fact, $(\mathbf{v} \cdot \nabla) f$ is simply the space derivative of f taken in the direction of $\mathbf{v}$ and weighted by the magnitude of $\mathbf{v}$.

An example of the application of (12.1.6), which will occur in Section 12.1.3 is the acceleration of a grain of matter moving in a velocity field $\mathbf{v}(x_1, x_2, x_3, t)$. According to (12.1.6),

$$\frac{D\mathbf{v}}{Dt} = \frac{\partial \mathbf{v}}{\partial t} + (\mathbf{v} \cdot \nabla)\mathbf{v}. \tag{12.1.7}$$

Example 12.1.1. As an example of the calculation of an acceleration, consider the velocity

$$\mathbf{v} = \frac{V_o}{a}(\mathbf{i}_1 x_2 - \mathbf{i}_2 x_1), \tag{a}$$

where V_o and a are positive constants. This will be recognized as the velocity of a fluid undergoing a rigid-body rotation about the x_3-axis. In fact, the angular velocity of the fluid is V_o/a, where $r = \sqrt{x_1^2 + x_2^2}$ is the radial distance from the x_3-axis. Note that $\partial \mathbf{v}/\partial t = 0$. Yet we know that the fluid is accelerating (centrifugal acceleration), and it is this acceleration that is given by the second term in (12.1.7), which becomes

$$\frac{D\mathbf{v}}{Dt} = (\mathbf{v} \cdot \nabla)\mathbf{v} = \left(v_1 \frac{\partial v_1}{\partial x_1} + v_2 \frac{\partial v_1}{\partial x_2}\right)\mathbf{i}_1 + \left(v_1 \frac{\partial v_2}{\partial x_1} + v_2 \frac{\partial v_2}{\partial x_2}\right)\mathbf{i}_2, \tag{b}$$

because v_3 and $\partial/\partial x_3$ are zero. Substitution of (a) into (b) gives

$$\frac{D\mathbf{v}}{Dt} = \left(\frac{V_o}{a}\right)^2 [-x_1(1)]\mathbf{i}_1 + [x_2(-1)]\mathbf{i}_2 \tag{c}$$

as the acceleration of the fluid. This acceleration is directed radially inward toward the x_3-axis and has the expected magnitude $(V_o/a)^2 r$ (the centrifugal acceleration).

We now obtain differential equations of motion that are appropriate for studying the dynamical behavior of incompressible inviscid fluids. We obtain the desired equations from two postulates:

1. Conservation of mass.
2. Conservation of momentum (Newton's second law).

The validity of these postulates has been verified by a variety of experiments.

12.1.2 Conservation of Mass

The conservation of mass states that mass can be neither created nor destroyed and thus must be conserved. To apply this postulate to a particular system consider the system of Fig. 12.1.1 in which an arbitrary volume V enclosed by the surface S is defined in a region containing material with a mass

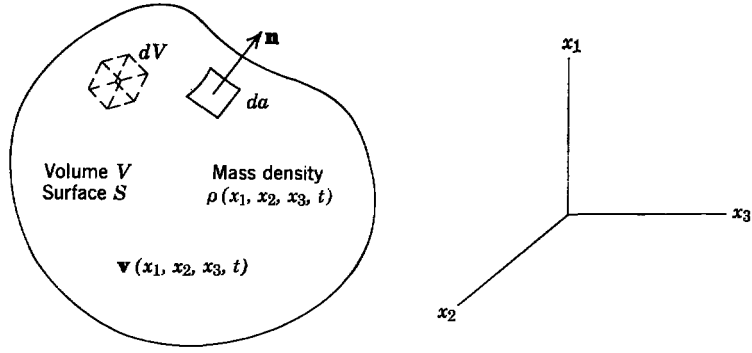

Fig. 12.1.1 Definition of system for writing conservation of mass.

density $\rho(x_1, x_2, x_3, t)$ (kg/m^3) and a velocity $\mathbf{v}(x_1, x_2, x_3, t)$ (m/sec). A differential volume element is dV, a differential surface element is da, and the normal vector $\mathbf{n}$ is normal to the surface and directed outward from the volume.

Because mass must be conserved, we can write the expression for the system in Fig. 12.1.1:

$$\oint_S (\rho \mathbf{v} \cdot \mathbf{n})\, da = -\frac{d}{dt}\int_V \rho\, dV. \tag{12.1.8}$$

The left side of this expression evaluates the net rate of mass flow (kg/sec) out of the volume V across the surface S. The right side indicates the rate at which the total mass within the volume decreases. Note the similarity between (12.1.8) and the conservation of charge described by (1.1.26)* in Chapter 1.

Example 12.1.2. The system in Fig. 12.1.2 consists of a pipe of inlet area A_i and outlet area A_o. A fluid of constant density ρ flows through the pipe. The velocity is assumed to be uniform across the pipe's cross section. The instantaneous fluid velocity at the inlet is

$$\mathbf{v}_i = \mathbf{i}_1 v_i$$

and is known. We wish to find the velocity $\mathbf{v}_o$ at the outlet.

We use the closed surface S indicated by dashed lines in Fig. 12.1.2 with the conservation of mass (12.1.8) to find $\mathbf{v}_o$. Because the density ρ is constant,

$$\oint_S (\mathbf{v} \cdot \mathbf{n})\, da = 0.$$

The only contributions to this integral come from the portions of the surface that coincide with the inlet and outlet. The result is

$$\oint_S (\mathbf{v} \cdot \mathbf{n})\, da = [\mathbf{v}_i \cdot (-\mathbf{i}_1)]A_i + (\mathbf{v}_o \cdot \mathbf{i}_1)A_o = 0$$

from which

$$\mathbf{v}_o = \mathbf{i}_1 v_o = \mathbf{i}_1 \frac{A_i}{A_o} v_i.$$

This expresses the intuitively apparent fact that in the steady state as much fluid leaves the closed surface S as enters it.

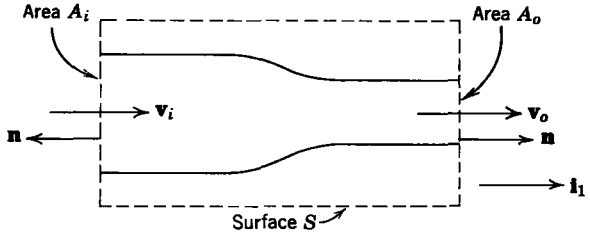

Fig. 12.1.2 Example for application of conservation of mass.

* Table 1.2, Appendix G.

We now write (12.1.8) in differential form by using the divergence theorem*

$$\oint_S (\mathbf{A} \cdot \mathbf{n})\, da = \int_V (\nabla \cdot \mathbf{A})\, dV$$

to change the surface integral in (12.1.8) to a volume integral

$$\int_V (\nabla \cdot \rho \mathbf{v})\, dV = -\int_V \frac{\partial \rho}{\partial t}\, dV. \tag{12.1.9}$$

The time derivative has been taken inside the integral sign because we assume that the volume V is stationary. This expression holds for any arbitrary volume V; therefore it must hold for a differential volume. Thus

$$\nabla \cdot \rho \mathbf{v} = -\frac{\partial \rho}{\partial t}, \tag{12.1.10}$$

which is the partial differential equation that describes the conservation of mass.

The left side of (12.1.10) can be expanded and the terms rearranged to obtain

$$\rho(\nabla \cdot \mathbf{v}) = -\frac{D\rho}{Dt}, \tag{12.1.11}$$

where the derivative on the right is the substantial derivative defined by (12.1.5). Equation 12.1.11 relates the rate of density decrease in a grain of matter to the divergence of the velocity and is in a form particularly useful when studying incompressible fluids because then the time rate of change of the density as viewed by a particle of fluid is zero, that is, $D\rho/Dt = 0$. Equation 12.1.11 indicates that in this case the velocity field has no divergence ($\nabla \cdot \mathbf{v} = 0$).

12.1.3 Conservation of Momentum (Newton's Second Law)

The second postulate of fluid mechanics is that Newton's second law of motion (conservation of momentum) must hold for each grain of matter. To express this postulate mathematically we assume that in the coordinate system (x_1, x_2, x_3) there exists a fluid of density $\rho(x_1, x_2, x_3, t)$ moving in a velocity field $\mathbf{v}(x_1, x_2, x_3, t)$. The mass of a grain of matter occupying the differential volume element $dx_1\, dx_2\, dx_3$ is $\rho\, dx_1\, dx_2\, dx_3$. We multiply this mass by the instantaneous acceleration found in (12.1.7) and equate the result to

* F. B. Hildebrand, *Advanced Calculus for Engineers*, Prentice-Hall, New York, 1948, pp. 312–315.

the total force **f** applied to the grain of matter*

$$\rho(dx_1\,dx_2\,dx_3)\left[\frac{\partial \mathbf{v}}{\partial t} + (\mathbf{v}\cdot\nabla)\mathbf{v}\right] = \mathbf{f}. \tag{12.1.12}$$

We now divide both sides of this expression by the volume element and define the force density **F** as

$$\mathbf{F} = \frac{\mathbf{f}}{dx_1\,dx_2\,dx_3} \tag{12.1.13}$$

to obtain the result

$$\rho\frac{D\mathbf{v}}{Dt} = \rho\frac{\partial \mathbf{v}}{\partial t} + \rho(\mathbf{v}\cdot\nabla)\mathbf{v} = \mathbf{F}. \tag{12.1.14}$$

This is the differential form of the conservation of momentum equation that we use most often in our treatment of continuum electromechanics.

The force density **F** in (12.1.14) can be written as

$$\mathbf{F} = \mathbf{F}^e + \rho\mathbf{g} + \mathbf{F}^m, \tag{12.1.15}$$

where $\mathbf{F}^e$ represents the electromagnetic forces that were expressed in various forms in Sections 8.1 and 8.3 of Chapter 8†, $\rho\mathbf{g}$ represents the force density resulting from gravity, and $\mathbf{F}^m$ represents mechanical forces applied to the grain of matter by adjacent material. This latter force density $\mathbf{F}^m$ depends on the physical properties of the fluid and will thus be described in Section 12.1.4 (on constituent relations).

Equation 12.1.14 can be expressed in a particularly simple and often useful form when we recognize that the force density on the right can be expressed as the space derivative of a stress tensor. We have already shown in Sections 8.1 and 8.3 of Chapter 8 that this is true. The ith component of the electromagnetic force density $\mathbf{F}^e$ is

$$F_i^e = \frac{\partial T_{ij}^e}{\partial x_j}, \tag{12.1.16}$$

where T_{ij}^e is the Maxwell stress tensor given for magnetic-field systems by (8.1.11)† and for electric field systems by (8.3.10)†. Because the gravitational field is conservative, we can write the gravitational force as the negative

* Newton's second law, written as $\mathbf{f} = M\mathbf{a}$, applies only for a mass M of fixed identity. Because $D\mathbf{v}/Dt$ is a derivative following a grain of matter, it is the acceleration of a set of mass particles ($\rho\,dx_1\,dx_2\,dx_3$) of fixed identity. Thus (12.1.12) is a valid description of Newton's second law written as $\mathbf{f} = M\mathbf{a}$ and is valid even when ρ is changing with space and time.

† See Table 8.1, Appendix G.

gradient of a scalar potential. We define the gravitational potential as U and write

$$\rho \mathbf{g} = -\nabla U, \tag{12.1.17}$$

or, in index notation, the ith component is

$$\rho g_i = -\frac{\partial U}{\partial x_i} = -\frac{\partial}{\partial x_j}(\delta_{ij} U). \tag{12.1.18}$$

We obtain the force density $\mathbf{F}^m$ of mechanical origin as the derivative of a stress tensor in Section 12.1.4 and therefore assume that the ith component of the mechanical force density $\mathbf{F}^m$ is

$$F_i^m = \frac{\partial T_{ij}{}^m}{\partial x_j}, \tag{12.1.19}$$

where $T_{ij}{}^m$ is the mechanical stress tensor to be calculated later.

Now the total stress tensor T_{ij} for the system is

$$T_{ij} = T_{ij}{}^e - \delta_{ij} U + T_{ij}{}^m, \tag{12.1.20}$$

and we can express the ith component of (12.1.14) simply as

$$\rho \frac{Dv_i}{Dt} = \frac{\partial T_{ij}}{\partial x_j}. \tag{12.1.21}$$

This form is particularly useful in applying boundary conditions.

Equation 12.1.14 is often useful when it is expressed in integral form. To achieve this end we multiply the conservation of mass (12.1.11) by the velocity $\mathbf{v}$ and add it to (12.1.14) to obtain

$$\rho \frac{D\mathbf{v}}{Dt} + \mathbf{v} \frac{D\rho}{Dt} + \rho \mathbf{v}(\nabla \cdot \mathbf{v}) = \mathbf{F}. \tag{12.1.22}$$

Because zero has been added to the left side of (12.1.14), (12.1.22) still expresses Newton's second law. Combination of the first two terms of (12.1.22) into the derivative of the product $(\rho \mathbf{v})$ and use of the definition of (12.1.6) leads to

$$\frac{\partial(\rho \mathbf{v})}{\partial t} + (\mathbf{v} \cdot \nabla)\rho \mathbf{v} + \rho \mathbf{v}(\nabla \cdot \mathbf{v}) = \mathbf{F}. \tag{12.1.23}$$

The ith component of this expression is

$$\frac{\partial(\rho v_i)}{\partial t} + (\mathbf{v} \cdot \nabla)\rho v_i + \rho v_i(\nabla \cdot \mathbf{v}) = F_i. \tag{12.1.24}$$

Combination of the second two terms on the left side of this expression yields

$$\frac{\partial(\rho v_i)}{\partial t} + (\nabla \cdot \rho v_i \mathbf{v}) = F_i. \tag{12.1.25}$$

We now integrate (12.1.25) throughout a volume V to obtain

$$\int_V \frac{\partial(\rho v_i)}{\partial t}\, dV + \int_V (\nabla \cdot \rho v_i \mathbf{v})\, dV = \int_V F_i\, dV. \tag{12.1.26}$$

The divergence theorem is used to change the second term on the left to an integral over the surface S that encloses the volume V and has the outward directed normal $\mathbf{n}$; thus

$$\int_V \frac{\partial(\rho v_i)}{\partial t}\, dV + \oint_S \rho v_i(\mathbf{v} \cdot \mathbf{n})\, da = \int_V F_i\, dV. \tag{12.1.27}$$

Using the definition of the total force density in terms of a stress tensor* in (12.1.21), we can also write (12.1.27) as

$$\int_V \frac{\partial(\rho v_i)}{\partial t}\, dV + \oint_S \rho v_i(v_j n_j)\, da = \oint_S T_{ij} n_j\, da. \tag{12.1.28}$$

Equation 12.1.27 can be written for each of the three components and then combined to obtain the vector form

$$\int_V \frac{\partial(\rho \mathbf{v})}{\partial t}\, dV + \oint_S \rho \mathbf{v}(\mathbf{v} \cdot \mathbf{n})\, da = \int_V \mathbf{F}\, dV. \tag{12.1.29}$$

This is the integral form of the equation that expresses conservation of momentum (Newton's second law).

The momentum density of the fluid is $\rho\mathbf{v}$; consequently, the first term on the left of (12.1.29) represents the time rate of increase of momentum density of the fluid that is instantaneously in the volume V. The second term gives the net rate at which momentum density is convected by the flow out of the volume V across the surface S. Thus the left side of (12.1.29) represents the *net* rate of increase of momentum in the volume V. The right side of (12.1.29) gives the net force applied to all the matter instantaneously in the volume V.

12.1.4 Constituent Relations

To complete the mathematical description of a fluid we must describe mathematically how the physical properties of the fluid affect the mechanical behavior. The physical properties of a fluid are described by constituent relations (equations of state), and the form of the equations depends on the fluid model to be used.

* See (8.1.13) and (8.1.17) of Appendix G.

A homogeneous, incompressible fluid, which is the model we are considering at present, has constant mass density, independent of other material properties (density and temperature) and of time. Thus one constituent relation is

$$\rho = \text{constant}. \tag{12.1.30}$$

This constituent relation is normally expressed in a different form by substituting (12.1.30) into (12.1.11) to obtain the equation

$$\nabla \cdot \mathbf{v} = 0, \tag{12.1.31}$$

which is the mathematical description normally used to express the property of incompressibility. Note, however [from (12.1.11)], that ρ does not have to be constant for (12.1.31) to hold. The fluid could be inhomogeneous and still be incompressible.

The next step in the description of physical properties is to determine how the mechanical force density $\mathbf{F}^m$ of (12.1.15) arises in a fluid.

First, consider a fluid at rest. By definition, a fluid at rest can sustain no shear stresses. Moreover, a fluid at rest can sustain only compressive stresses and a homogeneous, isotropic fluid will sustain the same compressive stress across a plane of arbitrary orientation. This isotropic compressive stress is defined as a positive hydrostatic pressure p.

We can define a mechanical stress tensor for the fluid at rest in the nomenclature of Sections 8.2 and 8.2.1*. Thus, because there are no shear stresses,

$$T_{ij}{}^m = 0, \quad \text{for} \quad i \neq j. \tag{12.1.32}$$

The normal stresses are all given by

$$T_{11}{}^m = T_{22}{}^m = T_{33}{}^m = -p. \tag{12.1.33}$$

The information contained in (12.1.32) and (12.1.33) can be written in compact form by using the Kronecker delta defined in (8.1.7) of Chap. 8*; therefore

$$T_{ij}{}^m = -\delta_{ij} p. \tag{12.1.34}$$

We can verify that the stress tensor in (12.1.34) describes an isotropic, normal compressive stress by calculating the traction* $\boldsymbol{\tau}^m$ applied to a surface of arbitrary orientation. To do this assume a surface with normal vector

$$\mathbf{n} = n_1\mathbf{i}_1 + n_2\mathbf{i}_2 + n_3\mathbf{i}_3. \tag{12.1.35}$$

Now use (8.2.2) of Chapter 8 with (12.1.34) and (12.1.35) to calculate the ith component of $\boldsymbol{\tau}^m$,

$$\tau_i{}^m = T_{ij}{}^m n_j = -p\,\delta_{ij} n_j = -p n_i \tag{12.1.36}$$

The vector traction then is

$$\boldsymbol{\tau}^m = -p(n_1\mathbf{i}_1 + n_2\mathbf{i}_2 + n_3\mathbf{i}_3) = -p\mathbf{n}. \tag{12.1.37}$$

* Appendix G.

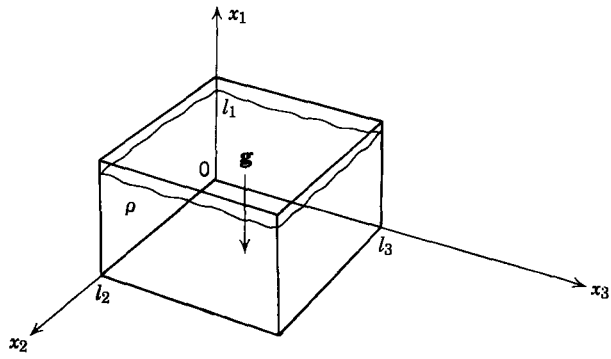

Fig. 12.1.3 Example for the application of stress tensor to a fluid at rest.

This traction is normal to the surface and in the direction opposite to the normal vector **n**. Thus the stress tensor of (12.1.34) describes an isotropic compressive stress.

The pressure p may be a function of position; consequently, a volume force density can result from a space variation of pressure. To find this force density we use (8.2.7)* to evaluate the ith component

$$F_i^m = \frac{\partial T_{ij}{}^m}{\partial x_j} = -\delta_{ij}\frac{\partial p}{\partial x_j} = -\frac{\partial p}{\partial x_i}. \tag{12.1.38}$$

When the three components are combined, the vector force density becomes

$$\begin{aligned} \mathbf{F}^m &= -\left(\frac{\partial p}{\partial x_1}\mathbf{i}_1 + \frac{\partial p}{\partial x_2}\mathbf{i}_2 + \frac{\partial p}{\partial x_3}\mathbf{i}_3\right) \\ \mathbf{F}^m &= -\nabla p. \end{aligned} \tag{12.1.39}$$

Example 12.1.3. As an example of the application of this mechanical force density, consider the system shown in Fig. 12.1.3 which consists of a container of lateral dimensions l_2 and l_3 and filled to a height l_1 with a fluid of constant mass density ρ. The acceleration of gravity **g** acts in the negative x_1-direction. The fluid is open to atmospheric pressure p_o at the top. We wish to find the hydrostatic pressure at any point in the fluid.

The fluid is at rest, so the acceleration is zero. Moreover, the only forces applied to the material are the force of gravity and the mechanical force from adjacent material. Thus the conservation of momentum (12.1.14) and (12.1.15) yields for this system

$$0 = -\mathbf{i}_1\rho g - \nabla p.$$

In component form this equation becomes

$$\begin{aligned} 0 &= -\rho g - \frac{\partial p}{\partial x_1}, \\ 0 &= -\frac{\partial p}{\partial x_2}, \\ 0 &= -\frac{\partial p}{\partial x_3} \end{aligned}$$

* See Appendix G.

We integrate these three equations to find that p is independent of x_2 and x_3 and is given in general by

$$p = -\rho g x_1 + C.$$

The integration constant C is determined by the condition that in the absence of surface forces the pressure must be continuous at $x_1 = l_1$. Thus

$$p = p_o + \rho g(l_1 - x_1).$$

Equations 12.1.34 and 12.1.39 describe mechanical properties of a fluid at rest. In a real fluid, motion will result in internal friction forces that add to the pressure force. In an *inviscid* fluid, however, motion results in no additional mechanical forces other than the forces of inertia already included in the momentum equation (12.1.14). Consequently, in the inviscid model the only mechanical force density [$\mathbf{F}^m$ in (12.1.15)] results from a space variation of pressure expressed by (12.1.39).

For an incompressible inviscid fluid the physical properties are completely specified by (12.1.31) and (12.1.39). Therefore, when boundary conditions and applied force densities (electrical and gravity) are specified, these constituent relations and (12.1.14) can be used to determine the motion of the fluid. We treat first some of the purely fluid-mechanical problems to identify the kinds of flow phenomena to be expected from this fluid model and then add electromechanical coupling terms.

12.2 MAGNETIC FIELD COUPLING WITH INCOMPRESSIBLE FLUIDS

An important class of electromechanical interactions is describable by irrotational flow; that is,

$$\nabla \times \mathbf{v} = 0. \tag{12.2.1}$$

When such an approximation is appropriate, the equations of motion can be solved quite easily because a vector whose curl is zero can be expressed as the gradient of a potential. Thus we define the class of problems for which (12.2.1) holds as *potential flow* problems and we define a *velocity potential* ϕ such that

$$\mathbf{v} = -\nabla\phi. \tag{12.2.2}$$

For incompressible flow $\nabla \cdot \mathbf{v} = 0$ from (12.1.31) and the potential ϕ must satisfy Laplace's equation

$$\nabla^2\phi = 0. \tag{12.2.3}$$

A solution of a potential flow problem then reduces to a solution of Laplace's equation that fits the boundary conditions imposed on the fluid.

We can now establish some important properties of potential flow. The momentum equation (12.1.14) takes the form

$$\rho \frac{\partial \mathbf{v}}{\partial t} + \rho(\mathbf{v} \cdot \nabla)\mathbf{v} = -\nabla p - \nabla U + \mathbf{F}^e, \tag{12.2.4}$$

where we have used the definition of the substantial derivative in (12.1.6) and the definition of the gravitational potential U in (12.1.17). The use of the vector identity

$$(\mathbf{v} \cdot \nabla)\mathbf{v} = \tfrac{1}{2}\nabla(v^2) - \mathbf{v} \times (\nabla \times \mathbf{v}),$$

where $v^2 = \mathbf{v} \cdot \mathbf{v}$, and (12.2.1) yields (12.2.4) in the alternative form

$$\rho \frac{\partial \mathbf{v}}{\partial t} + \tfrac{1}{2}\rho \nabla(v^2) = -\nabla p - \nabla U + \mathbf{F}^e. \tag{12.2.5}$$

We now use the facts that ρ is constant, that the space (∇) and time ($\partial/\partial t$) operators are independent, and that the velocity is expressed by (12.2.2) to write (12.2.5) in the form

$$\nabla\left(\rho \frac{\partial \phi}{\partial t} + \tfrac{1}{2}\rho v^2 + p + U\right) = \mathbf{F}^e. \tag{12.2.6}$$

By taking the curl of both sides of (12.2.6) we find that potential flow is possible only when

$$\nabla \times \mathbf{F}^e = 0. \tag{12.2.7}$$

If this condition is not satisfied, the assumption that $\nabla \times \mathbf{v} = 0$ is not valid.

Thus we restrict the treatment of the present section to electromechanical interactions in which the force density of electrical origin has no curl (12.2.7). In view of (12.2.7), we express the force density $\mathbf{F}^e$ as

$$\mathbf{F}^e = -\nabla \psi, \tag{12.2.8}$$

where ψ is an electromagnetic force potential, and write (12.2.6) as

$$\nabla\left(\rho \frac{\partial \phi}{\partial t} + \tfrac{1}{2}\rho v^2 + p + U + \psi\right) = 0. \tag{12.2.9}$$

The most general solution for this differential equation is

$$\rho \frac{\partial \phi}{\partial t} + \tfrac{1}{2}\rho v^2 + p + U + \psi = H(t); \tag{12.2.10}$$

that is, this expression can be a function of time but not a function of space.

When the flow is steady, $\partial\phi/\partial t = 0$ and none of the other quantities on the left of (12.2.10) is a function of time. Then (12.2.10) reduces to

$$\tfrac{1}{2}\rho v^2 + p + U + \psi = \text{constant}. \tag{12.2.11}$$

This result, known as *Bernoulli's equation*, expresses a constant of the motion and is useful in the solution of certain types of problem.

Example 12.2.1. As an example of the application of Bernoulli's equation, consider the system in Fig. 12.2.1. This system consists of a tank that is open to atmospheric pressure p_o and filled to a height h_1 with an inviscid, incompressible fluid. The fluid discharges through a small pipe at a height h_2 with velocity v_2. The area of the tank is large compared with the area of the discharge pipe; thus we assume that the tank empties so slowly that we can neglect the vertical velocity of the fluid and consider this as a steady flow problem.

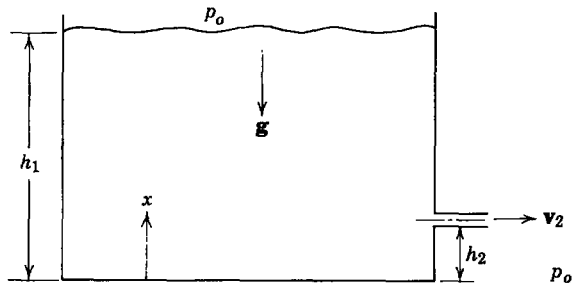

Fig. 12.2.1 Example of application of Bernoulli's equation.

There are no externally applied forces other than pressure and gravity, which has a downward acceleration g. We wish to find the discharge speed v_2.

The gravitational potential U is

$$U = \rho g x,$$

where we assume that x is measured from the bottom of the tank. (We could choose any other convenient reference point.)

Application of Bernoulli's equation (12.2.11) with $\psi = 0$ (there are no electromagnetic forces) at the top of the fluid and at the outlet of the discharge pipe yields

$$p_o + \rho g h_1 = p_o + \rho g h_2 + \tfrac{1}{2}\rho v_2^2,$$

from which

$$v_2 = \sqrt{2g(h_1 - h_2)}.$$

We now apply the equations of motion for potential flow to examples involving electromechanical coupling.

12.2.1 Coupling with Flow in a Constant-Area Channel

We first consider the flow of an incompressible inviscid fluid in a horizontal channel with the dimensions and coordinate system defined in Fig. 12.2.2. At the channel inlet ($x_1 = 0$) the fluid velocity is constrained to be

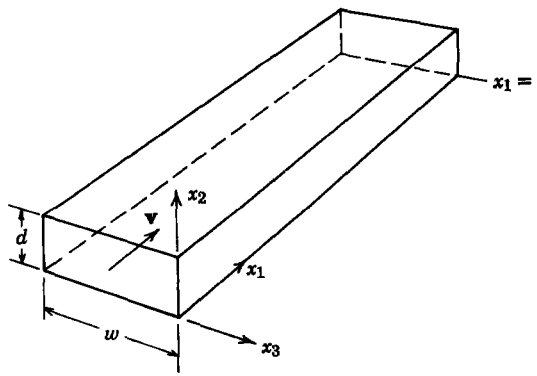

Fig. 12.2.2 A channel of constant cross-sectional area.

uniform and in the x_1-direction

$$\mathbf{v}(0, x_2, x_3, t) = \mathbf{i}_1 v_o(t). \tag{12.2.12}$$

At a fixed channel wall, the normal component of velocity must be zero and the tangential component is unconstrained (for an inviscid fluid); consequently, the velocity of flow throughout the channel is

$$\mathbf{v}(x_1, x_2, x_3, t) = \mathbf{i}_1 v_o(t) \tag{12.2.13}$$

and the velocity potential is

$$\phi(x_1, x_2, x_3, t) = -x_1 v_o(t). \tag{12.2.14}$$

Note that this potential satisfies Laplace's equation (12.2.3) and the boundary conditions.

Equation 12.2.13 is the velocity distribution in the constant-area channel with the boundary condition specified (12.2.12) regardless of the space distributions or time variations of applied force densities but with the restriction that these force densities be irrotational (12.2.7).

12.2.1a Steady-State Operation

In this section we analyze a simple coupled system that is the basic configuration for illustrating the most important phenomena in magnetohydrodynamic (MHD) conduction machines. In spite of the myriad factors (viscosity, compressibility, turbulence, etc.) that affect the properties of real devices, the model presented is used universally for making initial estimates of electromechanical coupling in MHD conduction machines of all types.

The basic configuration is illustrated in Fig. 12.2.3 and consists of a rectangular channel of length l, width w, and depth d, through which an electrically

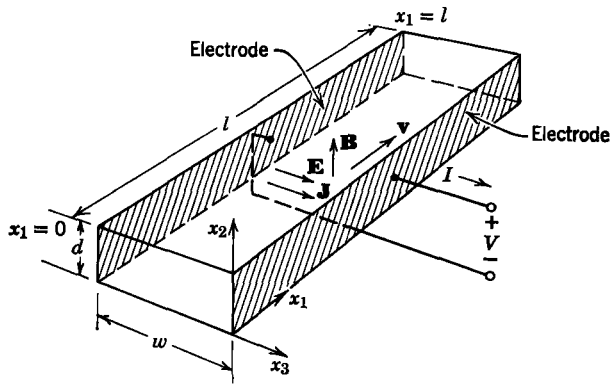

Fig. 12.2.3 Conduction-type, MHD machine.

conducting nonmagnetizable fluid flows with velocity $\mathbf{v}$ in the x_1-direction. The two channel walls perpendicular to the x_2-direction are insulators and the two walls perpendicular to the x_3-direction are highly conducting electrodes from which terminals are connected to an external circuit. The flux density $\mathbf{B}$ is in the x_2-direction and is produced by external coils or magnets not shown. The electrical conductivity σ of the fluid is high enough that the system can be modeled as a quasi-static magnetic field system.

We are considering an inviscid fluid model and we assume that the inlet ($x_1 = 0$) velocity is uniform as expressed by (12.2.12); thus the velocity is uniform throughout the channel as expressed by (12.2.13). We neglect fringing magnetic fields and the magnetic field due to current in the fluid* and assume that $\mathbf{B}$ is uniform:

$$\mathbf{B} = \mathbf{i}_2 B, \tag{12.2.15}$$

where B is constant. Because we are dealing with a steady-flow problem with time-invariant boundary conditions, $\partial/\partial t = 0$ and Faraday's law yields

$$\nabla \times \mathbf{E} = 0. \tag{12.2.16}$$

Once again we neglect fringing fields at the ends of the channel† and obtain the resulting solution

$$\mathbf{E} = -\mathbf{i}_3 \frac{V}{w}, \tag{12.2.17}$$

where V is the potential difference between the electrodes with the polarity defined in Fig. 12.2.3.

We now use Ohm's law for a moving conductor of conductivity σ (6.3.5),

$$\mathbf{J} = \sigma(\mathbf{E} + \mathbf{v} \times \mathbf{B}) \tag{12.2.18}$$

to write the current density for the system of Fig. 12.2.3 as

$$\mathbf{J} = \mathbf{i}_3 \sigma \left(-\frac{V}{w} + v_o B \right). \tag{12.2.19}$$

Note that this current density is uniform and therefore satisfies the conservation of charge condition $\nabla \cdot \mathbf{J} = 0$. Because the current density is uniform, it can

* The neglect of the self-field due to current in the fluid is justified for MHD generators when the magnetic Reynolds number based on channel length is much less than unity (see Section 7.1.2a).

† This assumption is quite good provided the l/w ratio of the channel is large (five or more). This result has been obtained in a detailed analysis of end effects by using a conformal mapping technique. The results of this analysis are presented in "Electrical and End Losses in a Magnetohydrodynamic Channel Due to End Current Loops," G. W. Sutton, H. Hurwitz, Jr., and H. Poritsky, Jr., *Trans. AIEE* (Comm. Elect.), **81**, 687–696 (January 1962).

be related to the terminal current by the area of an electrode; thus

$$\mathbf{J} = \mathbf{i}_3 \frac{I}{ld}. \tag{12.2.20}$$

To obtain the electrical terminal characteristics of this machine, we combine (12.2.19) and (12.2.20) to obtain

$$IR_i = -V + v_0 Bw, \tag{12.2.21}$$

where we have defined the internal resistance R_i as

$$R_i = \frac{w}{\sigma ld}. \tag{12.2.22}$$

Equation 12.2.21 can be represented by the equivalent circuit of Fig. 12.2.4. The open-circuit voltage ($v_0 Bw$) is generated by the motion of the conducting fluid through the magnetic field and has the same physical nature as speed voltage generated in conventional dc machines using solid conductors (see Section 6.4). This speed voltage can supply current to a load through the internal resistance R_i which is simply the resistance that would be measured between electrodes with the fluid at rest. From an electrical point of view the electromechanical interaction occurs in the equivalent battery ($v_0 Bw$) in Fig. 12.2.4.

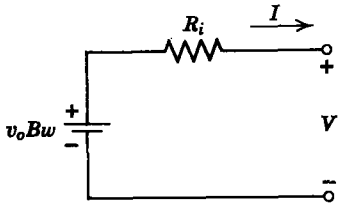

Fig. 12.2.4 Electrical equivalent circuit of conduction-type MHD machine.

To describe the properties of the MHD machine of Fig. 12.2.3, viewed from the electrical terminals, we have obtained a relation between terminal voltage and terminal current (12.2.21). From a mechanical point of view a similar relation is that between the pressure difference over the length of the channel and the velocity through the channel. This mechanical terminal relation is obtained from the x_1-component of the momentum equation (12.2.4):

$$0 = -\frac{\partial p}{\partial x_1} - \frac{IB}{ld}. \tag{12.2.23}$$

Integration of this equation over the length of the channel yields

$$\Delta p = -\frac{IB}{d}, \tag{12.2.24}$$

where the pressure rise Δp is defined by

$$\Delta p = p(l) - p(0). \tag{12.2.25}$$

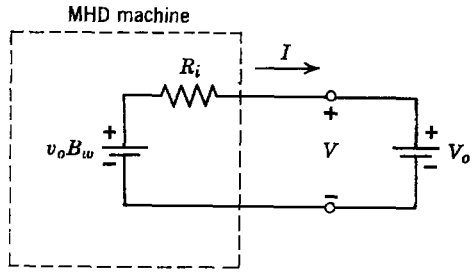

Fig. 12.2.5 MHD conduction machine with a constant-voltage constraint on the electrical terminals.

Equation 12.2.24 indicates that for this system the pressure rise along the channel is a function of the terminal current only and independent of the fluid velocity. This is reasonable because the pressure gradient is balanced by the $\mathbf{J} \times \mathbf{B}$ force density, regardless of the velocity. For an arbitrary electrical source or load the pressure rise will vary with velocity because the current depends on velocity through (12.2.21).

To study the energy conversion properties of the machine in Fig. 12.2.3 we constrain the electrical terminals with a constant-voltage source V_0 as indicated in Fig. 12.2.5 and study the behavior of the device as a function of the fluid velocity v_0. For this purpose we use (12.2.21) to find the current I as

$$I = \frac{v_0 Bw - V_0}{R_i} \tag{12.2.26}$$

Substitution of this result into (12.2.24) yields for the pressure rise

$$\Delta p = -\frac{B}{dR_i}(v_0 Bw - V_0). \tag{12.2.27}$$

The current and pressure rise are shown plotted as functions of velocity v_0 in Fig. 12.2.6.

To determine the nature of the device we define the electric power output P_e which, when positive, indicates a flow of electric energy from the MHD machine into the source V_0:

$$P_e = IV_0. \tag{12.2.28}$$

We also define the mechanical power out P_m, which represents power flow from the MHD machine into the velocity source v_0:

$$P_m = \Delta p w d v_0. \tag{12.2.29}$$

For the range of velocities

$$v_0 > \frac{V_0}{Bw}$$

we have

$$P_e > 0, \qquad P_m < 0$$

and the device is a generator; that is, mechanical power input is in part converted to electric power. For the velocity range

$$0 < v_o < \frac{V_o}{Bw}$$

we have

$$P_e < 0, \qquad P_m > 0$$

and the device is a pump. Electric power input is converted in part to mechanical power. For the velocity range

$$v_o < 0,$$

$$P_e < 0, \qquad P_m < 0;$$

that is, both mechanical and electrical power are into the MHD machine. All of this input power is dissipated in the internal resistance of the machine. In this region the machine acts as an electromechanical brake because electric

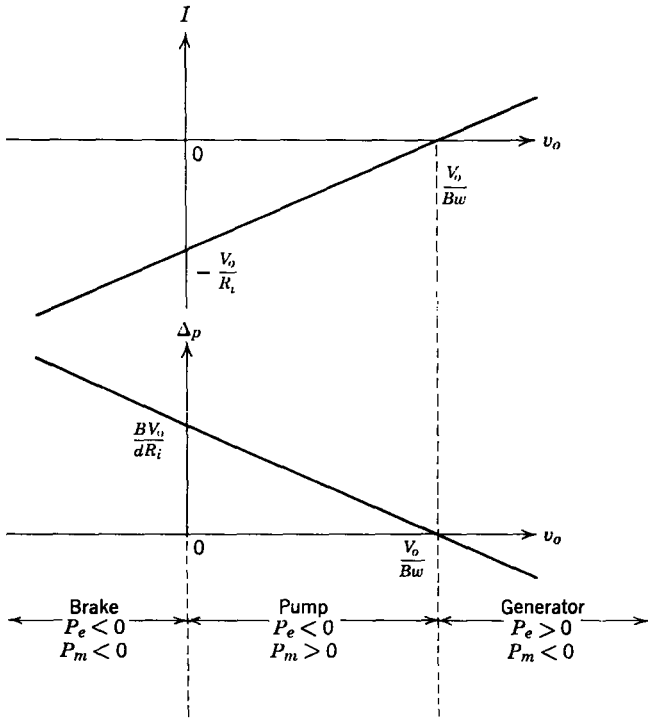

Fig. 12.2.6 Terminal characteristics of an MHD conduction-type machine with constant terminal voltage.

power is put in, and the only electromechanical result is to retard the fluid flow.

The properties of the MHD machine, as indicated by the curves of Fig. 12.2.6, can be interpreted in terms of the equivalent circuit of Fig. 12.2.5. We substitute (12.2.24) into (12.2.29) to find that the mechanical output power is expressible as

$$P_m = -I(v_0 Bw). \tag{12.2.30}$$

Reference to Fig. 12.2.5 shows that this is the power input to the battery that represents the speed voltage. Thus, when the battery ($v_0 Bw$) absorbs power, energy is being supplied to the velocity source by the MHD machine. When the battery ($v_0 Bw$) supplies power, energy is being supplied to the external voltage source by the MHD machine. When the battery ($v_0 Bw$) supplies power, energy is being extracted from the velocity source. Thus, when the two batteries of Fig. 12.2.5 have opposing polarities, energy can flow from one battery to the other and the machine can operate as a pump or a generator, the operation being determined by the relative values of the two battery voltages. When the polarities of both batteries are in the same direction ($v_0 < 0$ in Fig. 12.2.5), the two batteries supply energy to the resistance R_i, and the MHD machine acts as a sink for both electrical and mechanical energy. This is operation as a brake.

This analysis has been done for a particular set of terminal constraints. Essentially the same techniques can be used for other constraints. It is worthwhile to point out that (12.2.24) indicates that if the machine is constrained mechanically by a constant pressure source the electrical output will be at constant current.

The analysis just completed provides the basic model used in any examination of the electromechanical coupling process in conduction-type MHD devices, regardless of whether they are pumps or generators and whether the working fluid is a liquid or gas. The model and its consequences should be compared with those of commutator machines (Section 6.4.1) and of homopolar machines (Section 6.4.2). The similarities are evident and the opportunity of using the results of the analysis of one device for interpreting the behavior of another will broaden our understanding of electromechanical interactions of this kind.

An alternative method of achieving electromechanical coupling between an electrical system and a conducting fluid is to use a system that is analogous to the squirrel-cage induction machine analyzed in Section 4.1.6b. We shall not analyze this type of system here, but the analysis is a straightforward extension of concepts and techniques already presented. The system consists basically of a channel of flowing conducting fluid that is subjected to a transverse magnetic field in the form of a wave traveling in the direction of

flow. This wave is most often established by a distributed polyphase winding (Sections 4.1.4 and 4.1.7). When the wave of magnetic field travels faster than the fluid, the fluid is accelerated by the field and pumping action results. When the fluid travels faster than the magnetic field wave, the fluid is decelerated and electric power is generated. In the analysis of an induction machine magnetic diffusion and skin effect are important (Section 7.1.4).

Both conduction- and induction-type MHD machines are used for pumping liquid metals*; they are proposed for power generation with liquid metals† and used to accelerate ionized gases for space propulsion systems‡; both are proposed for power generation with ionized gases,§ although the conduction-type machine appears more attractive by far for this purpose.

12.2.1b Dynamic Operation

We now consider the kinds of phenomena that can result from electromechanical coupling with an incompressible fluid of time-varying velocity. We start by considering the fluid dynamic behavior of a simple example, which will then be the basis for a study of electromechanical transient effects.

The configuration to be studied is shown in Fig. 12.2.7. The system consists of a rigid tube of rectangular cross section bent into the form of a U. The depth d of the tube is small compared with the radius of the bends. The tube is filled with an incompressible inviscid fluid to a length l measured along the center of the tube. The two surfaces are open to atmospheric pressure p_o and gravity acts downward as shown.

It is clear that for static equilibrium the two surfaces of the fluid are at the same height. The displacement of the two surfaces from the equilibrium positions are designated x_a and x_b.

To study the dynamic behavior of this system we displace the fluid from equilibrium, release it from rest, and study the ensuing fluid motions.

The equations for solving this problem express conservation of mass and force equilibrium. Conservation of mass (12.1.31) used with the irrotational flow condition (12.2.1) and the fact that the channel has constant cross-sectional area leads to the conclusion that the flow velocity is uniform across the channel. (Here we ignore effects due to the channel curvature.)

* L. R. Blake, "Conduction and Induction Pumps for Liquid Metals," *Proc. Inst. of Elec Engrs. (London)*, **104A**, 49 (1957).

† D. G. Elliott, "Direct-Current Liquid Metal MHD Power Generation," *AIAA J.*, 627–634 (1966). M. Petrick and K. V. Lee, "Performance Characteristics of a Liquid Metal MHD Generator," *Intl. Symp. MHD Elec. Power Gen.*, Vol 2, pp. 953–965, Paris, July 1964.

‡ E. L. Resler and W. R. Sears, "The Prospects for Magnetohydrodynamics," *J. Aerospace Sci.*, **25**, No. 4, 235–245 (April 1958).

§ H. H. Woodson, "Magnetohydrodynamic AC Power Generation," *AIEE Pacific Energy Conversion Conf. Proc.*, pp. 30-1–30-2, San Francisco, 1964.

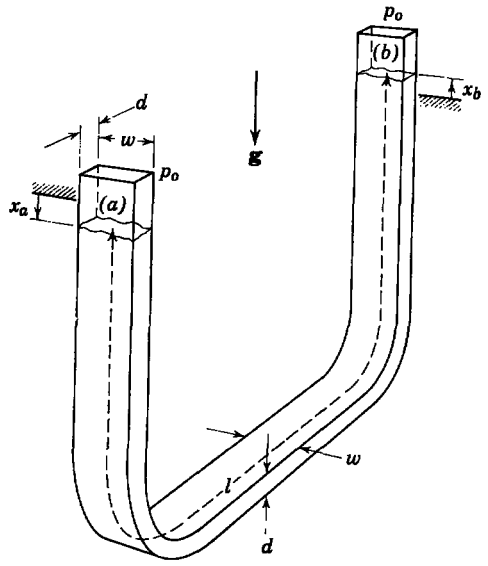

Fig. 12.2.7 Configuration for transient flow problem.

Furthermore, the displacements of the two surfaces are equal

$$x_a = x_b. \tag{12.2.31}$$

The form of the momentum equation that is most useful for this example is (12.2.5) with $\mathbf{F}^e = 0$.

$$\rho \frac{\partial \mathbf{v}}{\partial t} = -\nabla\left(p + \rho\frac{v^2}{2} + U\right), \tag{12.2.32}$$

where U is the gravitational potential. We now do a line integration of (12.2.32) from the surface at (a) to the surface at (b) along the center of the tube to obtain

$$\int_a^b \rho \frac{\partial \mathbf{v}}{\partial t} \cdot d\mathbf{l} = \int_a^b -\nabla\left(p + \rho\frac{v^2}{2} + U\right) \cdot d\mathbf{l} \tag{12.2.33a}$$

$$\rho l \frac{\partial v}{\partial t} = -2\rho g x_a. \tag{12.2.33b}$$

This result could have been obtained by using (12.2.10), a fact that is not surprising because the steps leading from (12.2.32) to (12.2.33) parallel those used in Section 12.2.

The velocity v is given by

$$v = \frac{dx_a}{dt};$$

thus we rewrite (12.2.33) as

$$l\frac{d^2x_a}{dt^2} + 2gx_a = 0, \tag{12.2.34}$$

which is a convenient expression for the surface displacement x_a. It shows that the dynamics are those of an undamped second-order system.

We now displace the fluid surface at (a) to the position

$$x_a(0) = X_o \tag{12.2.35}$$

and release it from rest

$$\frac{dx_a}{dt}(0) = 0. \tag{12.2.36}$$

The solution of (12.2.34) with the initial conditions of (12.2.35) and (12.2.36) is

$$x_a(t) = u_{-1}(t)X_o \cos \omega t, \tag{12.2.37}$$

where $u_{-1}(t)$ is the unit step and the frequency ω is given by

$$\omega = \left(\frac{2g}{l}\right)^{1/2}. \tag{12.2.38}$$

Note that this lossless, fluid-mechanical system has the basic property of a simple pendulum in that the natural frequency depends only on the acceleration of gravity and the length of fluid in the flow direction and is independent of the mass density of the fluid.

We now couple electromechanically to the system of Fig. 12.2.7 with an MHD machine of the kind analyzed in Section 12.2.1a placed in the U tube as shown in Fig. 12.2.8. The total length of fluid between the surfaces at (a) and (b) is still l and the length of the MHD machine in the flow direction is l_1. The flux density B is uniform over the length of the MHD machine and is again produced by a system not shown. As in Section 12.2.1a, we neglect the magnetic field due to current in the fluid as well as the end and edge effects. The terminals of the MHD machine are loaded with a resistance R.

In this analysis we are interested in the fluid dynamical transient that will usually be much slower than purely electrical transients whose time constant depends on the inductance of the electrode circuit. Thus we neglect the inductance of the electrode circuit and the electric terminal relation is obtained from (12.2.21) by setting

$$V = IR. \tag{12.2.39}$$

The resulting relation between current and velocity is

$$I = \frac{vBw}{R_i + R}, \tag{12.2.40}$$

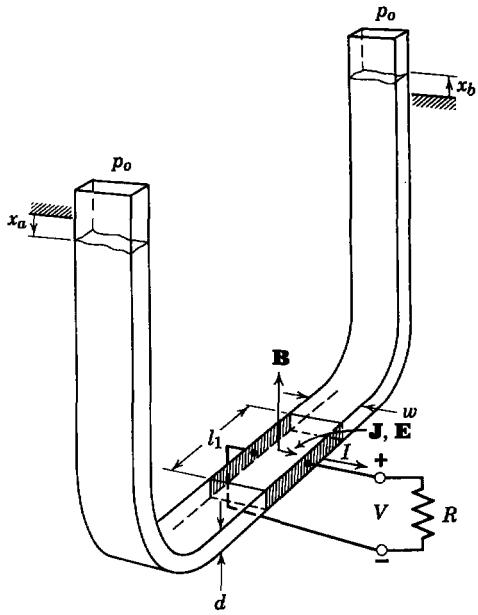

Fig. 12.2.8 Transient-flow problem with electromechanical coupling.

where the internal resistance is

$$R_i = \frac{w}{\sigma l_1 d}$$

and σ is the electrical conductivity of the fluid.

The addition of the electrical force term to the momentum equation (12.2.32) yields

$$\rho \frac{\partial \mathbf{v}}{\partial t} = -\nabla\left(p + \rho\frac{v^2}{2} + U\right) + \mathbf{J} \times \mathbf{B}. \tag{12.2.41}$$

Integration of this expression between the two fluid surfaces in the manner of (12.2.33) yields

$$\rho l \frac{\partial v}{\partial t} = -2\rho g x_a - \frac{IB}{d}. \tag{12.2.42}$$

Note that the last term on the right is simply the pressure rise through the MHD machine due to the electromagnetic force density (12.2.24).

Substitution of (12.2.40) and $v = dx_a/dt$ into (12.2.42) yields the differential equation in x_a

$$\rho l \frac{d^2x_a}{dt^2} + \frac{B^2 w}{d(R_i + R)}\frac{dx_a}{dt} + 2\rho g x_a = 0. \tag{12.2.43}$$

Comparison of (12.2.43) with (12.2.34) shows that the electromechanical coupling with a resistive load has added a damping term to the differential equation. This is easily understandable in terms of the analysis of the MHD machine in Section 12.2.1a. The fluid motion produces a voltage proportional to speed, a resistive load on this voltage produces a current proportional to speed, and the current in the fluid interacts with the applied flux density to produce a retarding force proportional to speed. Thus the electrical force appears as a damping term in the differential equation.

To consider the kind of behavior that can result in a real system of this kind we assume that the fluid is mercury, which has the following constants

$$\rho = 13{,}600 \text{ kg/m}^3, \qquad \sigma = 10^6 \text{ mhos/m}.$$

The system dimensions are chosen to be

$$l = 1 \text{ m}, \qquad l_1 = 0.1 \text{ m},$$
$$w = 0.02 \text{ m}, \qquad d = 0.01 \text{ m}.$$

We set the load resistance R equal to the internal resistance R_i

$$R = R_i = 2 \times 10^{-5} \, \Omega.$$

For these given constants the differential equation (12.2.43) reduces to

$$\frac{d^2x_a}{dt^2} + 3.68B^2 \frac{dx_a}{dt} + 19.6x_a = 0. \tag{12.2.44}$$

When the fluid is released from rest with the initial conditions of (12.2.35) and (12.2.36), the resulting transients in fluid position and electrode current are shown in Fig. 12.2.9. It is clear that with attainable flux densities the electromechanical coupling force can provide significant damping for the system.*

Some properties of the curves of Fig. 12.2.9 are worth noting. First, for very small time ($t < 0.1$ sec) the response in fluid position is essentially unaffected by the force of electric origin. This occurs because the initial velocity is zero and it takes velocity to generate voltage and drive current. Thus the initial increase in velocity is independent of the value of flux density and the initial current buildup is proportional to flux density.

The resistive load on the electrodes of the MHD machine in Fig. 12.2.8 can be replaced by an electrical source and the fluid displacement can be driven electrically. In such a case, when the fluid motion is of interest, (12.2.21) and (12.2.42) are adequate for the study.

* An experiment to demonstrate this effect is complicated by the fact that the contact resistance between the liquid metal and the electrodes is likely to be appreciable.

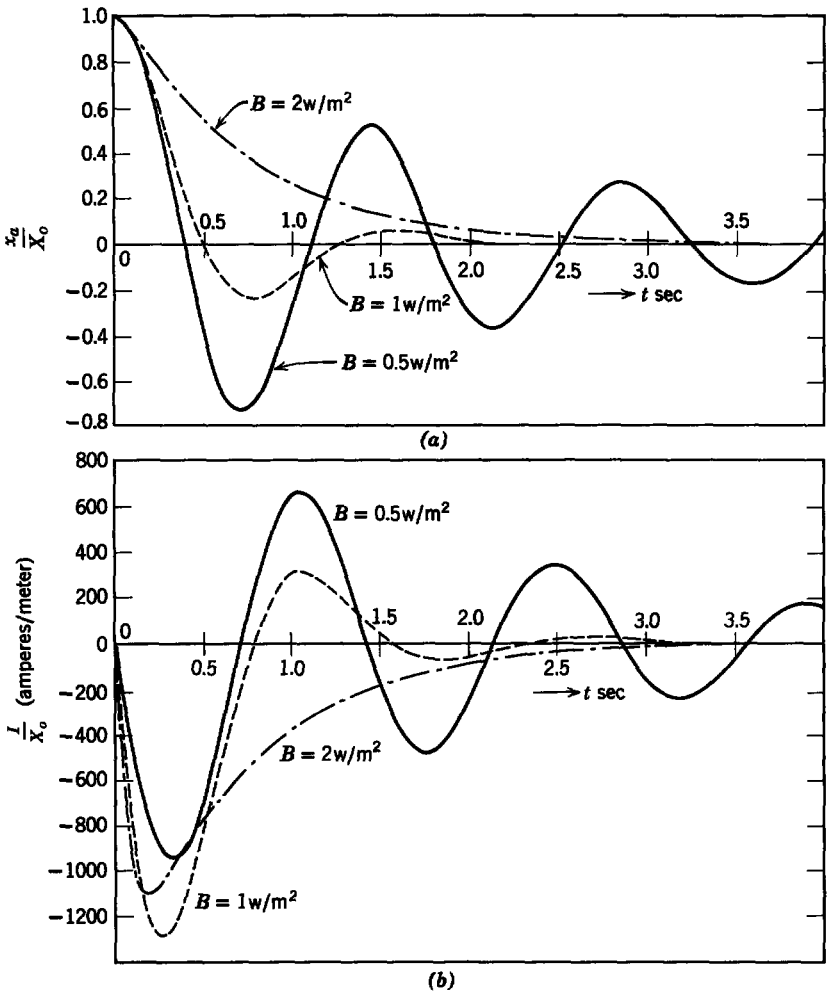

Fig. 12.2.9 Transient response of MHD-damped system: (*a*) fluid position; (*b*) electrode current.

12.2.2 Coupling with Flow in a Variable-Area Channel

To establish some insight into the properties of potential flow in two dimensions, consider the flow around a corner in the configuration of Fig. 12.2.10. The fluid container has constant depth in the x_3-direction and the fluid is incompressible and inviscid. There are no electrical forces, and we neglect gravity effects (assume gravity to act in the x_3-direction).

For potential flow the velocity is given by (12.2.2) as $\mathbf{v} = -\nabla\phi$ and the velocity potential ϕ satisfies Laplace's equation ($\nabla^2\phi = 0$). The boundary

condition is that the normal component of velocity must be zero along the rigid surfaces. The solution of Laplace's equation which satisfies these boundary conditions is

$$\phi = \frac{v_o}{\sqrt{2}a}(x_2^2 - x_1^2), \tag{12.2.45}$$

where $2v_o$ is the speed of the fluid at $x_1 = x_2 = a$. The velocity is thus given by

$$\mathbf{v} = \mathbf{i}_1\sqrt{2}\,v_o\frac{x_1}{a} - \mathbf{i}_2\sqrt{2}\,v_o\frac{x_2}{a}. \tag{12.2.46}$$

Equipotential lines and streamlines are shown in Fig. 12.2.10. This solution is valid, even if v_o is time-varying.

We now restrict our attention to a steady-flow problem (v_o = constant) and find that Bernoulli's equation (12.2.11) yields

$$\tfrac{1}{2}\rho v^2 + p = \text{constant}. \tag{12.2.47}$$

We note from (12.2.46) that at $x_1 = x_2 = 0$ the velocity $\mathbf{v} = 0$. Because the velocity is zero, this is called a *stagnation point*. If we designate the pressure at the stagnation point as p_o, (12.2.47) becomes

$$\tfrac{1}{2}\rho v^2 + p = p_o. \tag{12.2.48}$$

Thus with a knowledge of the stagnation point pressure and the velocity distribution we can find the pressure at any other point in the fluid. The use of

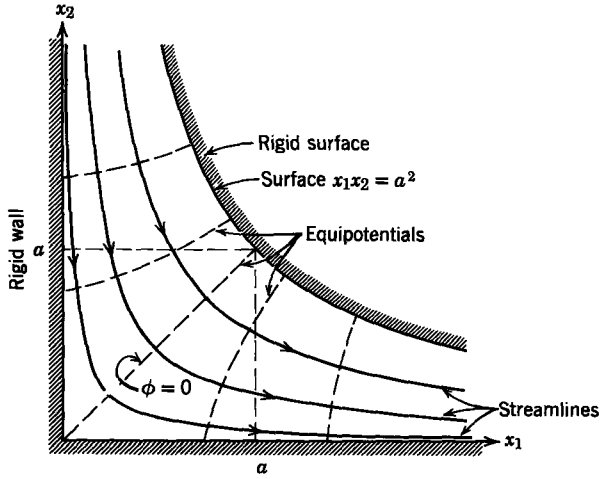

Fig. 12.2.10 Example of potential flow.

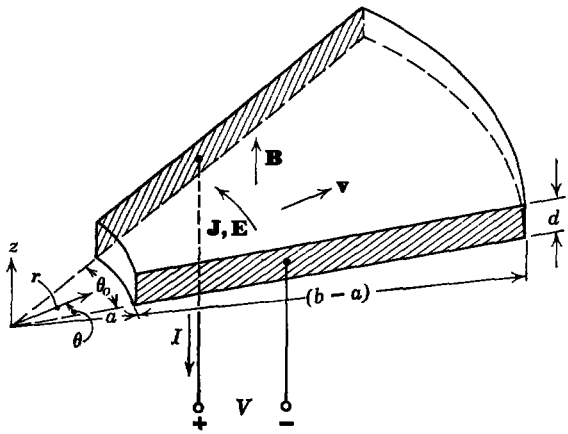

Fig. 12.2.11 MHD conduction machine with variable area.

(12.2.46) in (12.2.48) yields for the pressure at point (x_1, x_2)

$$p = p_o - \frac{\rho v_o^2}{a^2}(x_1^2 + x_2^2). \tag{12.2.49}$$

From this result we conclude that in a flowing incompressible fluid the highest pressure occurs at the stagnation point. Moreover, for a given flow the higher the local fluid speed, the lower the local pressure.*

This example indicates that the pressure can be changed by changing the velocity and vice versa. Variations of velocity are obtained by varying the cross-sectional area of the fluid flow. We now do an example of an MHD interaction with a two-dimensional fluid flow in which the geometry of the channel can be adjusted to vary the relation between input pressure and velocity and output pressure and velocity. Such freedom is desirable in many MHD applications. Here it allows us to extend the basic ideas introduced in Section 12.2.1a to a case in which the fluid is accelerating but the flow is steady ($\partial/\partial t = 0$).

The system to be considered is the conduction machine shown schematically in Fig. 12.2.11. The channel forms a segment of a cylinder. The inlet is at radius $r = a$ and the outlet is at radius $r = b$. The insulating walls perpendicular to the z-direction are separated by a distance d. The electrodes are in radial planes separated by the angle θ_o. We use a cylindrical coordinate system r, θ, z, defined in Fig. 12.2.11. There is an applied flux density **B** in

* Even though (12.2.49) indicates that the pressure p can go negative, in fact it cannot. As long as we use an incompressible model, the pressure appears in only one place in the equations of motion, and they remain unaltered if an arbitrary constant is added to (or subtracted from) p. Other effects, such as compressibility, depend on an equation of state that is sensitive to the absolute magnitude of the pressure. If these effects are included, a negative pressure is not physically possible.

the z-direction. The electrodes are connected to electrical terminals at which the voltage V and current I are defined.

The velocity at the inlet ($r = a$) and the velocity at the outlet ($r = b$) are assumed to be radial and constant in magnitude. We assume solutions with cylindrical symmetry. These solutions are quite accurate, provided the angle θ_o is reasonably small. Again the magnetic field generated by current in the fluid is neglected (low magnetic Reynolds number).

As already assumed, the fluid is incompressible and inviscid with electrical conductivity σ and permeability μ_0. The velocity is radial

$$\mathbf{v} = \mathbf{i}_r v_r \tag{12.2.50}$$

and the electric field intensity and current density are azimuthal

$$\mathbf{E} = \mathbf{i}_\theta E_\theta, \tag{12.2.51}$$

$$\mathbf{J} = \mathbf{i}_\theta J_\theta. \tag{12.2.52}$$

We have already specified that the total flux density is

$$\mathbf{B} = \mathbf{i}_z B_z, \tag{12.2.53}$$

where B_z is a constant.

We first assume that at the inlet ($r = a$) the radial component of velocity is

$$v_r = v_a. \tag{12.2.54}$$

Next, conservation of mass for incompressible flow requires that

$$\oint_S \mathbf{v} \cdot \mathbf{n}\, da = 0. \tag{12.2.55}$$

The value of v_r at any radius r follows as

$$v_r = \frac{a}{r} v_a. \tag{12.2.56}$$

Steady-state operation yields $\nabla \times \mathbf{E} = 0$ and the z-component of $\nabla \times \mathbf{E} = 0$ [assuming that $\mathbf{E}$ takes the form of (12.2.51)] is

$$\frac{1}{r} \frac{\partial (rE_\theta)}{\partial r} = 0. \tag{12.2.57}$$

This yields the result that

$$E_\theta = \frac{A}{r}, \tag{12.2.58}$$

where A is a constant to be determined from the boundary conditions. To evaluate the constant A, the definition of the terminal voltage

$$-\int_0^{\theta_o} E_\theta r\, d\theta = V \tag{12.2.59}$$

is used to obtain

$$E_\theta = -\frac{V}{r\theta_o}. \tag{12.2.60}$$

Substitution of (12.2.53), (12.2.56), and (12.2.60) into the θ-component of Ohm's law for a moving, conducting medium (12.2.18) yields

$$J_\theta = \sigma\left(-\frac{V}{r\theta_o} + \frac{a}{r}v_a B_z\right). \tag{12.2.61}$$

Note that this expression satisfies $\nabla \cdot \mathbf{J} = 0$.

A relation between current density and terminal current can be obtained from the expression

$$I = \int_a^b J_\theta d\, dr. \tag{12.2.62}$$

Performance of this integration yields

$$IR_i = -V + a\theta_o v_a B_z, \tag{12.2.63}$$

where we have defined the internal resistance R_i as

$$R_i = \frac{\theta_o}{\sigma d \ln (b/a)} \tag{12.2.64}$$

Note the similarity between (12.2.63) and (12.2.21) for the simpler geometry in Fig. 12.2.3.

The radial component of the momentum equation (12.2.4) for steady-state conditions is

$$\rho v_r \frac{\partial v_r}{\partial r} = -\frac{\partial p}{\partial r} + J_\theta B_z. \tag{12.2.65}$$

Multiplication of the expression by dr, integration from $r = a$ to $r = b$, and use of (12.2.56) and (12.2.62) yields

$$\tfrac{1}{2}\rho v_a^2\left[\left(\frac{a}{b}\right)^2 - 1\right] = -\Delta p - \frac{IB_z}{d}, \tag{12.2.66}$$

where the pressure rise Δp is defined as

$$\Delta p = p(b) - p(a). \tag{12.2.67}$$

Note the similarity between (12.2.66) and (12.2.24) for the constant-area channel. The difference lies in the first term on the left of (12.2.66) which results from the changing area and therefore changing velocity in the channel of Fig. 12.2.11.

Equation 12.2.66 could have been obtained from Bernoulli's equation (12.2.11); in a simple case like this, however, it is more informative to obtain the result from first principles.

To study some of the properties of the system with varying area consider first the case in which the electrical terminals are open-circuited. The terminal voltage, as obtained from (12.2.63) is

$$V = a\theta_o v_a B_z \tag{12.2.68}$$

and the pressure rise obtained from (12.2.66) is

$$\Delta p = \tfrac{1}{2}\rho v_a^2\left[1 - \left(\frac{a}{b}\right)^2\right]. \tag{12.2.69}$$

Because $a < b$, this pressure rise is positive, which indicates that the outlet pressure is higher than the inlet pressure. This results because the fluid velocity decreases as r increases and this fluid deceleration must be balanced by a pressure gradient as indicated by the momentum equation (12.2.65). Thus the variable area channel by itself acts as a kind of "fluid transformer" that can increase pressure as it decreases velocity or vice versa.

The electrical terminal relation (12.2.63) for the machine with variable area (Fig. 12.2.11) has the same form as the electrical terminal relation (12.2.21) for the machine with constant area (Fig. 12.2.3). Thus, if the inlet velocity v_a is the independent mechanical variable, the analysis of the electric terminal behavior is exactly the same as that of the constant-area machine; that is, from an electrical point of view the machine appears to have an open-circuit voltage ($a\theta_o v_a B_z$) in series with an internal resistance R_i (12.2.64), as illustrated in Fig. 12.2.12. This equivalent circuit can be connected to any combination of active and passive loads, and the electrical behavior can be predicted correctly within the limitations of the assumptions made in arriving at the model.

To study the energy conversion properties of the variable-area machine we must generalize the concept of mechanical input power that was used in (12.2.29) for the constant-area machine. No longer is the mechanical input power simply equal to the pressure difference times the volume flow rate of fluid because the difference in inlet and outlet velocities indicates that there is

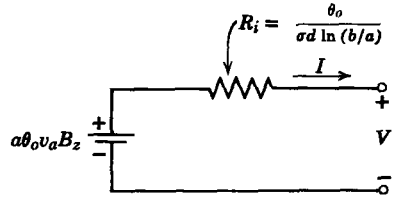

Fig. 12.2.12 Electric equivalent circuit for a variable-area MHD machine.

a net transport of kinetic energy into or out of the volume of the channel by the fluid. To illustrate this concept consider the system operating with the electrical terminals open-circuited. There is clearly no electrical output power and no I^2R_i losses in the fluid. Moreover, the fluid is inviscid, so there can be no mechanical losses. Thus we expect the mechanical input power to be zero, although there is a nonzero pressure difference between inlet and outlet of the channel.

To determine the mechanical energy interchange between the MHD device and the energy source which makes the fluid flow through the device we use the *conservation of energy* which states, in general,

$$\begin{bmatrix}\text{total power input}\\ \text{to channel volume}\end{bmatrix}=\begin{bmatrix}\text{rate of increase of}\\ \text{energy stored in volume}\end{bmatrix} \tag{12.2.70}$$

For the steady-state problem being considered the energy stored in the volume is constant and the right side of (12.2.70) is zero. We thus define the mechanical *output* power from the channel as P_m and the power converted to electrical form as P_{em} and write (12.2.70) for conservation of *mechanical* energy* as

$$-P_m - P_{em} = 0. \tag{12.2.71}$$

For open-circuit conditions the electromechanical power P_{em} is zero and

$$P_m = 0. \tag{12.2.72}$$

To calculate P_m, which has been defined as the work done by the fluid in the channel *on* the fluid mechanical source, we must specify how work is done on the fluid in the channel and how energy is stored and transported by the fluid.

At a surface of a fluid (this can be an imaginary surface in a fluid) with outward directed normal vector $\mathbf{n}$, as illustrated in Fig. 12.2.13, there will be a pressure force on the fluid enclosed by the surface of magnitude p and directed opposite to the normal vector $(-p\mathbf{n})$ [see (12.1.37)]. If the fluid is moving with velocity $\mathbf{v}$ at the surface, the rate at which the pressure force $(-p\mathbf{n}\,da)$ does work on the fluid inside the volume V is

$$\begin{bmatrix}\text{power input from}\\ \text{pressure forces}\end{bmatrix}=\oint_S -p\mathbf{n}\cdot\mathbf{v}\,da. \tag{12.2.73}$$

A fluid can store kinetic energy with a density $\frac{1}{2}\rho v^2$. At each point along the surface of Fig. 12.2.13 fluid flow across the surface will transport kinetic energy into or out of the volume V. The volume of fluid crossing the surface

* Even though electrical losses in the fluid (I^2R_i) occur within the volume of the channel, they are not included in this energy expression. This is possible here because these losses do not affect the mechanical properties of an incompressible, inviscid fluid. When we consider gaseous conductors in Chapter 13, the electrical losses must be included because they will affect the mechanical properties of the conducting fluid.

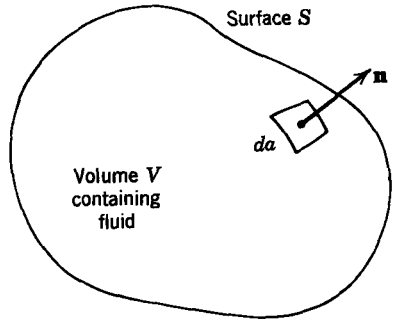

Fig. 12.2.13 Geometry for writing conservation of energy for a fluid.

element da in unit time is $\mathbf{v} \cdot \mathbf{n}\, da$. Thus the total kinetic energy transported out of the volume in unit time is

$$\begin{bmatrix}\text{power output from kinetic} \\ \text{energy transport}\end{bmatrix} = \oint_S \tfrac{1}{2}\rho v^2 \mathbf{v} \cdot \mathbf{n}\, da. \tag{12.2.74}$$

For an incompressible inviscid fluid (12.2.73) and (12.2.74) represent the only mechanisms for interchanging mechanical energy with a fluid; thus the mechanical output power P_m defined in (12.2.71) is given by

$$P_m = \oint_S p\mathbf{n} \cdot \mathbf{v}\, da + \oint_S \tfrac{1}{2}\rho v^2 \mathbf{v} \cdot \mathbf{n}\, da. \tag{12.2.75}$$

To apply (12.2.75) to the variable-area channel of Fig. 12.2.11 we must define the surface that encloses the fluid in the channel. This surface consists of the four channel walls and the two concentric cylindrical surfaces at $r = a$ and $r = b$. The velocity is nonzero only along the last two surfaces; consequently, (12.2.75) integrates to

$$P_m = -p(a)v_r(a)a\theta_o d + p(b)v_r(b)b\theta_o d - \tfrac{1}{2}\rho v_r^3(a)a\theta_o d + \tfrac{1}{2}\rho v_r^3(b)b\theta_o d. \tag{12.2.76}$$

The assumption that $v_r(a) = v_a$ (12.2.54) and the use of (12.2.56) to write

$$v_r(b) = \frac{a}{b} v_a \tag{12.2.77}$$

allows us to write (12.2.76) in the simplified form

$$P_m = a\theta_o d v_a \left[\Delta p - \tfrac{1}{2}\rho v_a^2 \left(1 - \frac{a^2}{b^2}\right)\right], \tag{12.2.78}$$

where the pressure rise Δp has been defined in (12.2.67) as $\Delta p = p(b) - p(a)$.

To apply (12.2.78) we first note that for the open-circuit condition $I = 0$, and (12.2.66) yields

$$\Delta p_{oc} = \tfrac{1}{2}\rho v_a^2\left(1 - \frac{a^2}{b^2}\right). \tag{12.2.79}$$

Substitution of this result into (12.2.78) yields for open-circuit conditions

$$P_m = 0.$$

This is in agreement with our intuitive physical prediction made at the start of this development. Next, for any arbitrary load $I \neq 0$ (12.2.66) yields

$$\Delta p = \tfrac{1}{2}\rho v_a^2\left(1 - \frac{a^2}{b^2}\right) - \frac{IB_z}{d}. \tag{12.2.80}$$

Substitution of this result into (12.2.78) and simplification yield

$$P_m = -a\theta_o v_a B_z I. \tag{12.2.81}$$

From (12.2.71) the power converted electromechanically is

$$P_{em} = -P_m = a\theta_o v_a B_z I. \tag{12.2.82}$$

Reference to the equivalent circuit of Fig. 12.2.12 shows that this converted power is simply the power supplied to the electric circuit by the battery representing the open-circuit voltage.

This interpretation leads to the conclusion that for conversion of energy the variable-area machine has exactly the same properties as the constant-area machine analyzed earlier. The only difference arises when we are interested in the details of the pressure and velocity distributions and in the nature of the fluid mechanical source that provides the fluid flow through the machine. As we shall see in Chapter 13, however, these are essential considerations if the velocity is large enough (compared with that of sound) to make the effects of compressibility important.

12.2.3 Alfvén Waves

So far in the treatment of electromechanical coupling with incompressible inviscid fluids we have considered problems in which there has been gross motion of the fluid. All of these examples have been analyzed by using potential flow. In this section we consider electromechanical coupling that results in no gross motion of the fluid but rather involves the propagation of a signal through a fluid. Moreover, the fluid velocity has a finite curl and a potential flow model is inappropriate. Our discussion is pertinent to an understanding of MHD transient phenomena.

As discussed in Section 12.1.4, an inviscid, incompressible fluid can, by itself, support no shear stresses; but when such a fluid with very high

electrical conductivity is immersed in a magnetic field the magnetic field provides shear stiffness such that transverse waves, called Alfvén waves and very much akin to the shear waves in elastic media, can be propagated. They play an essential role in determining the dynamics of a highly conducting liquid or gas (plasma) interacting with a magnetic field.

To introduce the essential features of Alfvén waves we use a rectangular system in which variables are functions of only one dimension. It is difficult to realize physically the boundary conditions necessary for this model. Thus, after the ideas are introduced, we extend the example to cylindrical geometry, where all boundary conditions can be imposed realistically.

The magnetohydrodynamic system is shown in Fig. 12.2.14. An incompressible, inviscid, highly conducting ($\sigma \to \infty$) fluid is contained between rigid parallel walls. An external magnet is used to impose a magnetic flux density B_o in the x_1-direction. It is the effect of this flux density on the motions of the fluid transverse to the x_1-axis that is of interest.

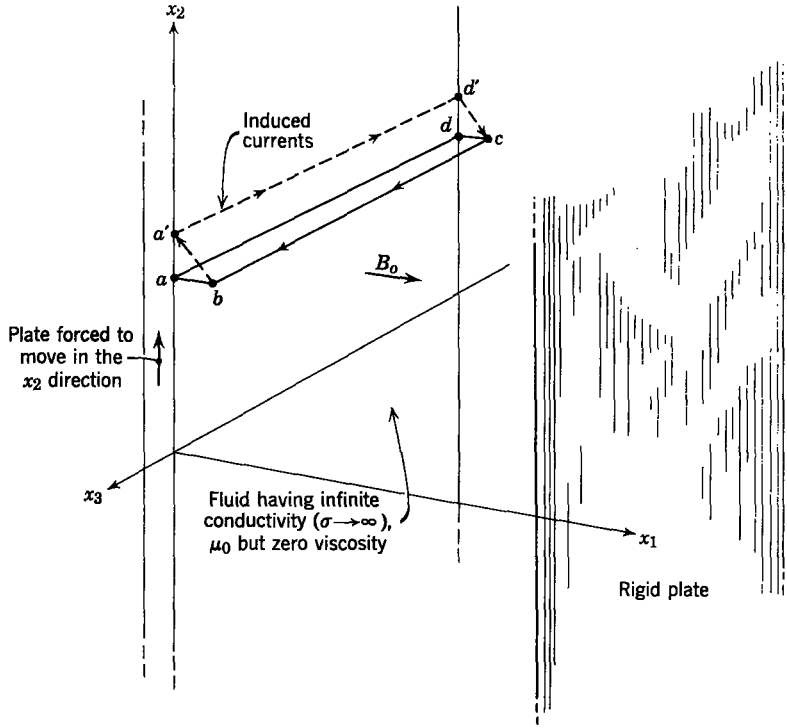

Fig. 12.2.14 Fluid contained between rigid parallel plates and immersed in a magnetic induction B_o. Motions of the fluid are induced by transverse motions of the left-hand plate, which, like the fluid, is assumed to be highly conducting.

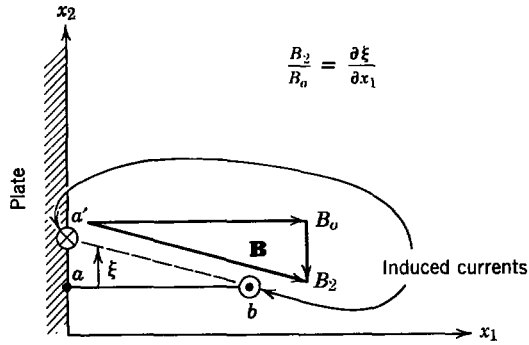

Fig. 12.2.15 End view of the loop *abcd* shown in Fig. 12.2.14. The initial loop formed by conducting fluid and the plate links zero flux λ. To conserve the flux, density **B** remains tangential to the loop with the additional magnetic flux density B_2 created by an induced current.

Suppose that in the absence of a magnetic field the rigid plate is set in motion in the x_2-direction. Because the fluid is inviscid, there is no shearing stress imposed on the fluid and the plate will transmit no motion to the fluid. In fact, if any sheet of fluid perpendicular to the x_1-axis is set into transverse motion, the adjacent sheets of fluid remain unaffected because of the lack of shearing stresses.

Now consider the effect of imposing a magnetic field. The fluid is highly conducting, and this means that the electric field in the frame of the fluid is essentially zero. The law of induction can be written for a contour C attached to the fluid particles:

$$\oint_C \mathbf{E}' \cdot d\mathbf{l} = -\frac{d}{dt}\int_S \mathbf{B} \cdot \mathbf{n}\, da \equiv -\frac{d\lambda}{dt}, \tag{12.2.83}$$

where $\mathbf{E}'$ is the electric field measured in the frame of the fluid.* Because the first integral is zero, the flux λ linked by a conduction path always made up of the same fluid particles remains constant.

This is an important fact for the situation shown in Fig. 12.2.14, as can be seen by considering the conduction path *abcd* intersecting the fluid and the edge of the rigid plate at $x_1 = 0$. Initially the surface enclosed by this path is in the x_2-x_3 plane, hence links no flux ($\lambda = 0$). When the plate is forced to move in the x_2-direction this surface, which is always made up of the same material particles, moves to $a'bcd'$. Because the surface is tilted, there is now a flux from B_0 that contributes to λ. Because λ must remain zero, however, there is a current induced around the loop in such a direction that it cancels the flux contributed by B_0. There is then an addition to the magnetic field (induced by this current) along the x_2-axis (Fig. 12.2.15) that makes the net

* See (1.1.23), Table 1.2, Appendix G.

magnetic field remain tangential to the surface of the deformed loop. This is necessary if λ is to remain zero.

The current, returning along the path *cb* in the fluid flows transverse to the field B_o; hence there is a magnetic force on the fluid ($\mathbf{J} \times B_o\mathbf{i}_1$) in the x_2-direction. The result of moving the highly conducting plate in the x_2-direction is a motion of the fluid adjacent to the plate in the same direction. The motion of the plate creates a magnetic shearing stress on the fluid. This stress is transmitted through the fluid in the x_1-direction because the magnetic force sets the fluid in the plane of *bc* into motion, and this sheet of fluid now plays the role of the plate in inducing motions in the neighboring sheets of fluid.

In our arguments we have assumed that motions of the fluid are the same at all points in a given x_2-x_3 plane. To provide an analytical picture of the dynamics consistent with this assumption it is assumed that all variables are independent of x_2 and x_3. As an immediate consequence of this assumption, the condition that $\nabla \cdot \mathbf{B} = 0$ requires that B_o be independent of x_1. If, in addition, B_o is imposed by an external magnet driven by a constant current, it follows that $B_1 = B_o =$ constant, regardless of the fluid motions. By similar reasoning the incompressible nature of the fluid ($\nabla \cdot \mathbf{v} = 0$), together with the rigid walls that do not permit flow along the x_1-axis, require that $v_1 = 0$ everywhere in the fluid. Hence both the fluid motions and additions to the magnetic flux density occur transverse to the x_1-axis.

From the discussion that has been given it is clear that three essential ingredients in the fluid motions are of interest here. First, a mathematical model must account for the law of induction. In particular, since the magnetic field is induced in the x_2-direction, we write the x_2-component of the induction equation

$$\frac{\partial E_3}{\partial x_1} = \frac{\partial B_2}{\partial t}. \tag{12.2.84}$$

The second important effect comes from the high conductivity of the fluid. In order that the conduction current may remain finite in the limit in which the conductivity σ becomes large, we must require that $\mathbf{E}' = 0$. This in turn means that $\mathbf{E} = -\mathbf{v} \times \mathbf{B}$, and it is the x_3-component of this equation that is of interest to us:

$$E_3 = v_2 B_o. \tag{12.2.85}$$

Substitution of this expression for E_3 into (12.2.84) gives an equation that expresses the effect of the fluid deformation on the magnetic field.

$$B_o \frac{\partial v_2}{\partial x_1} = \frac{\partial B_2}{\partial t} \tag{12.2.86}$$

Note that if we define a transverse particle displacement in the fluid such that $v_2 = \partial\xi/\partial t$ (12.2.86) simply requires that the magnetic flux density remain

tangential to the deformed surface of fluid initially in a given x_1-x_3 plane. Equation 12.2.86 shows that the lines of magnetic field intensity are deformed as though they were "frozen" to the particles of fluid (see Fig. 12.2.15).

The third input to our analytical description comes from the effect of the magnetic field on the fluid motions. Because the fluid moves in the x_2-direction, we write the x_2-component of the force equation (12.1.21)

$$\rho \frac{\partial v_2}{\partial t} = \frac{\partial T_{21}}{\partial x_1} = \frac{B_o}{\mu_0} \frac{\partial B_2}{\partial x_1}. \tag{12.2.87}$$

Note that the absence of a velocity component v_1 and the one-dimensional character of the motions under consideration eliminate the spatial derivatives from the substantial derivative (the first term) in this expression. The only component of the Maxwell stress tensor* that enters on the right is T_{21} because variables do not depend on x_2 or x_3 and we have made use of the fact that B_o is a constant in writing Eq. 12.2.87.

The last two equations can be used to write an expression for either B_2 or v_2; for example, we eliminate B_2 between the time derivative of (12.2.87) and the space derivative of (12.2.86) to obtain

$$\frac{\partial^2 v_2}{\partial t^2} = \frac{B_o^2}{\mu_0 \rho} \frac{\partial^2 v_2}{\partial x_1^2}, \tag{12.2.88}$$

where

$$a_b = \left(\frac{B_o^2}{\mu_0 \rho}\right)^{1/2}.$$

This is the wave equation, considered in some detail in Chapters 9 and 10. The velocity a_b with which waves propagate in the x_1-direction is called the Alfvén velocity.†

To develop further a physical feel for the nature of an Alfvén wave, consider the propagation in the positive x_1-direction of the pulse illustrated in Fig. 12.2.16. The pulse, as drawn, represents what happens along the x_1-axis; but, because in our model the variables are independent of x_2 and x_3, the figure applies to all elements having the same coordinate x_1. With reference to Fig. 12.2.16, we can easily show that the variables as sketched satisfy (12.2.86) and (12.2.87) with **J** found by Ampère's law. Moreover, (12.2.88) is satisfied when the waveforms maintain constant shape and propagate in the x_1-direction with the Alfvén velocity a_b.

We note from Fig. 12.2.16 that the force density $\mathbf{J} \times \mathbf{B}$ has an x_2-component equal to $J_3 B_o$ and that this force density is in the positive x_2-direction in the leading half of the wave and in the negative x_2-direction in the trailing half of the wave. Thus, as the wave propagates in the x_1-direction, the fluid at the

* Table 8.1, Appendix G.

† Alfvén waves are named after the man who first recognized their significance for astrophysics. See H. Alfvén, *Cosmical Electrodynamics*, Oxford, 1950.

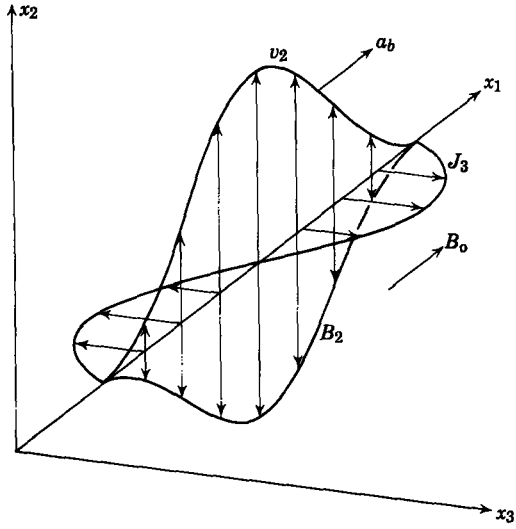

Fig. 12.2.16 The variables associated with an Alfvén wave.

leading edge is accelerated upward by the electrical force and at the trailing edge the fluid is decelerated.

It is instructive to use the pulse of Fig. 12.2.16 to construct the curves of Fig. 12.2.17 which show the displacement of the fluid particles that were initially on the x_1-axis. Fluid particles and magnetic flux lines are displaced in the same way by the passage of the Alfvén wave. For a highly conducting ($\sigma \to \infty$) fluid the fluid particles and magnetic flux lines are "frozen" together and any motion of the fluid causes a distortion of the flux lines.

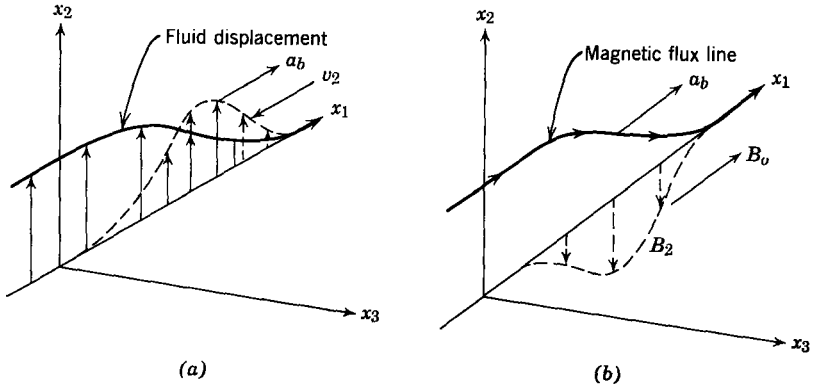

Fig. 12.2.17 Fluid displacement and flux-line distortion in an Alfvén wave: (*a*) fluid displacement; (*b*) magnetic flux line.

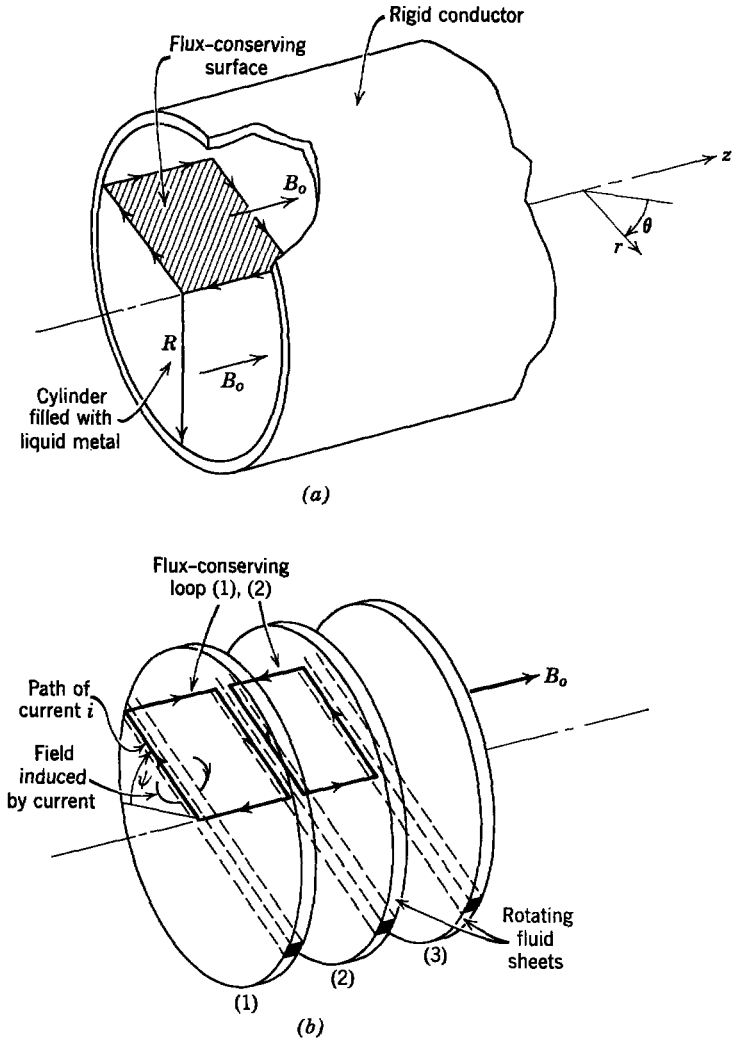

Fig. 12.2.18 (*a*) Experimental arrangement for producing torsional Alfvén waves in highly conducting cylindrical container; (*b*) conduction paths represented as "spokes" in adjacent wheels of perfectly conducting fluid.

It would be difficult to generate Alfvén waves in the cartesian geometry of Fig. 12.2.14 for two reasons. First, fluid motions in the x_2-direction have been assumed independent of x_2 and this implies that container boundaries in x_1-x_3 planes must not inhibit the velocity v_2. Second, currents that flow along the x_3-axis must have a return path ($\nabla \cdot \mathbf{J} = 0$), and this implies that conducting walls are provided by the container in x_1-x_2 planes. We can satisfy both requirements by using the cylindrical container shown in Fig. 12.2.18. Here

we expect that Alfvén waves will appear as torsional motions of the fluid about the axis of the cylinder. These motions, like those just considered, are transverse to the imposed magnetic field B_0 (which has the same direction as the axis of the cylinder).

Again it is helpful to think of the fluid as composed of sheets, as shown in Fig. 12.2.18. Now the sheets take the form of wheels that can execute torsional motions about the cylinder axis. Currents can flow radially outward along "spokes" of a "wheel" through the outer cylinder wall, inward along another "spoke," and finally complete the loop along the cylinder axis (Fig. 12.2.18). In fact, these loops provide a simple picture of the electromechanical mechanism responsible for the propagation of waves along the magnetic field B_0.

Suppose that the first slice of fluid is forced to rotate to the positive angle ψ (Fig. 12.2.18*b*). The loop formed by the conducting path through the neighboring sheet initially links no flux. To conserve this condition in spite of the rotation a current i is induced which tends to cancel the flux caused by B_0. This current returns to the center through the neighboring sheet. In doing so it produces a force density $\mathbf{J} \times \mathbf{B}_0$ which tends to rotate this second sheet in the positive ψ-direction. Of course, as the second sheet rotates, a current must flow around a loop through the third sheet to conserve the zero flux condition in the second loop of Fig. 12.2.18. Hence the third sheet of fluid is set into motion and the initial rotation propagates along the cylinder axis. These arguments can be repeated for motions that propagate in the opposite direction. The waves have no polarity and can propagate in either direction along the lines of magnetic field B_0 The propagation is not instantaneous because each sheet has a finite mass and time is required to set the fluid in motion

The magnetic field has the same effect on the fluid as if the fluid sheets were interconnected by taut springs (Fig. 12.2.19). Wave propagation occurs

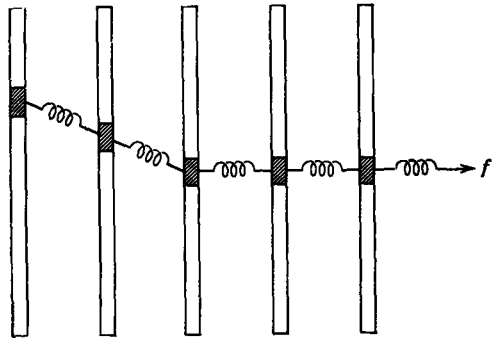

Fig. 12.2.19 Side view of the circular sheets of fluid in Fig. 12.2.18 showing equivalent interconnecting springs under the tension f.

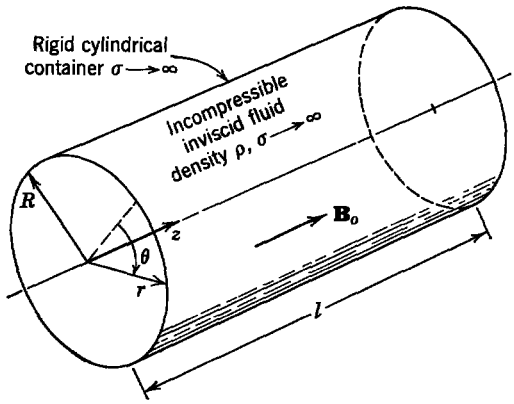

Fig. 12.2.20 Cylindrical geometry for the study of Alfvén waves.

very much as it does on a string (Section 9.2.). In the string the wave velocity was proportional to the square root of the tension f*. Here the tension is apparently proportional to B^2, as can be seen by comparing (12.2.88) and (9.2.4). This would be expected from a simple experiment: hold one sheet fixed and twist the next sheet and there is a restoring torque proportional to f. With the magnetic field the restoring torque is caused by $\mathbf{J} \times \mathbf{B}_0$, but since J is induced in proportion to B_0 this magnetic restoring torque is proportional to B_0^2. Hence we can think of B_0^2 as producing a magnetic tension in a perfectly conducting fluid.

To be precise about the fluid velocity and electrical current distribution, we now consider a specific analytical example. The system, illustrated in Fig. 12.2.20, consists of a rigid, cylindrical container made of highly conducting material, filled with a highly conducting fluid, and immersed in an equilibrium axial flux density $\mathbf{B}_0$ produced externally. The ends of the cylinder are also rigid and may be insulators or conductors, depending on the boundary conditions desired. The fluid is modeled as incompressible and inviscid with mass density ρ, permeability μ_0, and high electrical conductivity ($\sigma \to \infty$). The fluid in the cylinder has axial length l and radius R. We use the cylindrical coordinate system illustrated in Fig. 12.2.20.

We specify that any drive will be applied at the ends and will have cylindrical symmetry; that is, there will be no variation with the angle θ and $\mathbf{v} = \mathbf{i}_\theta v_\theta(r, z, t)$. In this case we can require that the relevant variables have only the following components, defined in terms of the cylindrical coordinate system (r, θ, z) in Fig. 12.2.20.

$$\mathbf{B} = \mathbf{i}_z B_0 + \mathbf{i}_\theta B_\theta, \tag{12.2.89}$$

$$\mathbf{J} = \mathbf{i}_r J_r + \mathbf{i}_z J_z, \tag{12.2.90}$$

$$\mathbf{E} = \mathbf{i}_r E_r + \mathbf{i}_z E_z. \tag{12.2.91}$$

* See Table 9.2, Appendix G.

The variables v_θ, B_θ, J_r, J_z, E_r, and E_z can be functions of r, z, and time t.

To analyze this system we must write the necessary equations in cylindrical coordinates by recognizing that $(\partial/\partial\theta) = 0$. For the basic equations refer to Table 1.2*, and for their forms in cylindrical coordinates refer to any standard text on electromagnetic theory.† The use of the constituent relation $\mathbf{B} = \mu_0\mathbf{H}$ with Ampère's law (1.1.1)* in cylindrical coordinates yields

$$-\frac{1}{\mu_0}\frac{\partial B_\theta}{\partial z} = J_r, \tag{12.2.92}$$

$$\frac{1}{\mu_0 r}\frac{\partial}{\partial r}(rB_\theta) = J_z. \tag{12.2.93}$$

We obtain from Faraday's law (1.1.5)

$$\frac{\partial E_r}{\partial z} - \frac{\partial E_z}{\partial r} = -\frac{\partial B_\theta}{\partial t}. \tag{12.2.94}$$

Ohm's law (12.2.18) yields

$$J_r = \sigma(E_r + v_\theta B_o), \tag{12.2.95}$$

$$J_z = \sigma E_z, \tag{12.2.96}$$

with J_r and J_z related by the condition of conservation of charge (1.1.3)*

$$\frac{1}{r}\frac{\partial}{\partial r}(rJ_r) + \frac{\partial J_z}{\partial z} = 0. \tag{12.2.97}$$

The θ-component of the momentum equation (12.1.14) with $\mathbf{F}^e = \mathbf{J} \times \mathbf{B}$ is

$$\rho\frac{\partial v_\theta}{\partial t} = -J_r B_o. \tag{12.2.98}$$

We now assume high conductivity ($\sigma \to \infty$), which, coupled with the fact that $\mathbf{J}$ remains finite, reduces (12.2.95) and (12.2.96) to

$$E_r = -v_\theta B_o, \tag{12.2.99}$$

$$E_z = 0. \tag{12.2.100}$$

These expressions are used in 12.2.94 to write

$$B_o\frac{\partial v_\theta}{\partial z} = \frac{\partial B_\theta}{\partial t}. \tag{12.2.101}$$

* See Table 1.2, Appendix G.

† See, for example, R. M. Fano, L. J. Chu, and R. B. Adler, *Electromagnetic Fields, Energy, and Forces*, Wiley, New York, 1960, p. 510.

Equations 12.2.92, 12.2.98, and 12.2.101 are combined to obtain the wave equation

$$\frac{\partial^2 v_\theta}{\partial t^2} = \frac{B_o^2}{\mu_0 \rho} \frac{\partial^2 v_\theta}{\partial z^2}. \tag{12.2.102}$$

This equation indicates that waves can propagate in the z-direction with the Alfvén velocity [see (12.2.88)].

$$a_b = \left(\frac{B_o^2}{\mu_0 \rho}\right)^{1/2}. \tag{12.2.103}$$

Note that (12.2.102) has no derivatives with respect to the radius r although the variables may be functions of r as indicated by (12.2.93) and (12.2.97). Variations with r are determined by boundary conditions; for instance, the general solution of (12.2.102) can be written in the separable form as

$$v_\theta = A(r) f(z, t). \tag{12.2.104}$$

The function $A(r)$ is then set by boundary conditions and automatically satisfies all the differential equations.

To consider a specific example of boundary conditions we assume that the end of the container at $z = 0$ is rigid, fixed, and made of insulating material ($\sigma \to 0$). The end at $z = l$ is highly conducting ($\sigma \to \infty$) and is rotated about its axis with a velocity

$$v_p = \text{Re}\,(\Omega r e^{j\omega t}). \tag{12.2.105}$$

These constraints impose the following boundary conditions:

$$\text{at } z = 0, \qquad J_z = 0 \tag{12.2.106}$$

$$\text{at } z = l, \qquad v_\theta = \text{Re}\,(\Omega r e^{j\omega t}). \tag{12.2.107}$$

This last boundary condition reflects the fact that there can be no slip between the perfectly conducting moving wall and the adjacent fluid because of the magnetic field; that is, the electric field must remain continuous across this boundary. Since $\mathbf{E} = -\mathbf{v} \times \mathbf{B}$ and the normal $\mathbf{B}$ is continuous across the boundary, it follows that the fluid velocity must also be continuous.

The solution for v_θ can now be assumed to have the form

$$v_\theta = \text{Re}\,[A(r)\hat{v}_\theta(z)\, e^{j\omega t}]. \tag{12.2.108}$$

Substitution of this assumed solution into (12.2.102) yields the differential equation

$$\frac{d^2 \hat{v}_\theta}{dz^2} = -k^2 \hat{v}_\theta, \tag{12.2.109}$$

where

$$k = \frac{\omega}{a_b}.$$

The solution of this equation is, in general,

$$\hat{v}_\theta = C_1 \cos kz + C_2 \sin kz. \tag{12.2.110}$$

Imposing the boundary condition at $z = l$, (12.2.107) yields

$$\Omega r = A(r)(C_1 \cos kl + C_2 \sin kl). \tag{12.2.111}$$

To maintain $A(r)$ nondimensional as indicated by (12.2.108), while satisfying this last equation for all values of r, we set

$$A(r) = \frac{r}{R} \tag{12.2.112}$$

and rewrite (12.2.111) as

$$\Omega R = C_1 \cos kl + C_2 \sin kl. \tag{12.2.113}$$

To apply the boundary condition at $z = 0$ we need to find an expression for J_z. We accomplish this by first substituting (12.2.108) into (12.2.101) to obtain

$$\frac{\partial B_\theta}{\partial t} = \text{Re}\left[B_o A(r) \frac{d\hat{v}_\theta}{dz} e^{j\omega t}\right]. \tag{12.2.114}$$

If we assume that

$$B_\theta = \text{Re}\,[A(r)\hat{B}_\theta(z)e^{j\omega t}], \tag{12.2.115}$$

then, using (12.2.114), we obtain

$$j\omega \hat{B}_\theta(z) = B_o \frac{d\hat{v}_\theta}{dz}, \tag{12.2.116}$$

which, by using (12.2.110), yields

$$\hat{B}_\theta(z) = \frac{B_o k}{j\omega}(-C_1 \sin kz + C_2 \cos kz). \tag{12.2.117}$$

Now we use (12.2.93) to evaluate J_z as

$$J_z = \text{Re}\left[\frac{2B_o k}{j\omega\mu_0 R}(-C_1 \sin kz + C_2 \cos kz)e^{j\omega t}\right]. \tag{12.2.118}$$

The boundary condition at $z = 0$ (12.2.106) now requires

$$C_2 = 0. \tag{12.2.119}$$

We use this result with (12.2.113) to find

$$C_1 = \frac{\Omega R}{\cos kl}. \tag{12.2.120}$$

The resulting solutions are

$$v_\theta = \text{Re}\left(\Omega r \frac{\cos kz}{\cos kl} e^{j\omega t}\right), \tag{12.2.121}$$

$$B_\theta = \text{Re}\left(-\frac{\Omega r B_0 k}{j\omega} \frac{\sin kz}{\cos kl} e^{j\omega t}\right), \tag{12.2.122}$$

$$J_z = \text{Re}\left(-\frac{2\Omega B_0 k}{\omega \mu_0} \frac{\sin kz}{\cos kl} e^{j\omega t}\right), \tag{12.2.123}$$

$$J_r = \text{Re}\left(-\frac{j\omega \rho \Omega r}{B_0} \frac{\cos kz}{\cos kl} e^{j\omega t}\right). \tag{12.2.124}$$

Study of these solutions indicates that there are standing, torsional waves in the system. The fluid motion is azimuthal and the flux line distortion is azimuthal. The details of the phenomena involved in the wave propagation are as described in connection with Fig. 12.2.18. Now, however, we see that the current loops are distributed throughout the fluid.

Because Alfvén waves are reflected from both ends of the container, the system exhibits an infinite number of resonances whose frequencies are defined by

$$\cos kl = 0. \tag{12.2.125}$$

The boundary condition at the insulated end of the cylinder (12.2.106) is essentially a free end condition. This is true because no current can flow in the insulator and no electrical forces are available at the boundary to perturb the fluid motion. Also, because the fluid is inviscid, there can be no tangential mechanical force applied to the fluid by the end plate. At the perfectly conducting end plate ($z = l$) the fluid "sticks" to the end plate because of electrical forces. A small radial current loop with one side in the end plate and the other side in the fluid will keep the flux linking it at zero. This produces the currents that interact with B_0 to allow no slippage of the fluid at a perfectly conducting boundary that is perpendicular to the equilibrium flux density.

To ascertain the kinds of numbers that would be involved in an experimental system of this sort, consider a container with the dimensions

$$l = 0.1 \text{ m}, \qquad R = 0.1 \text{ m}.$$

Assume the fluid to be liquid sodium (sometimes used as a coolant for nuclear reactors) which has a mass density, at 100°C, of

$$\rho = 930 \text{ kg/m}^3.$$

If we assume a flux density of

$$B_0 = 1 \text{ Wb/m}^2,$$

which is easily obtainable with iron-core electromagnets, we obtain an Alfvén velocity of

$$a_h = 31 \text{ m/sec.}$$

The lowest resonance frequency of this system is given from (12.2.125) by

$$k = \frac{\pi}{2l},$$

which yields

$$\omega = 490 \text{ rad/sec}$$

or

$$f = 78 \text{ Hz.}$$

From these results we can see that Alfvén waves propagate at low velocities in liquid metals and that for devices of reasonable size the resonance frequencies also are low.

In our treatment of Alfvén waves we have assumed that the electrical conductivity of the fluid is infinite. In such a case we wonder how the flux density B_0 can exist in the fluid. The answer is simply that the conductivity is large but finite, and in establishing the equilibrium conditions sufficient time was allowed for the flux density B_0 to be established by diffusion into the fluid. In the analysis of the waves the assumption $\sigma \to \infty$ means simply that the diffusion time of the magnetic field through the fluid is much longer than the time required for the wave to propagate through the fluid* (see Section 7.1).

We have introduced Alfvén waves by using an incompressible fluid model. These waves can also propagate in compressible, highly conducting fluids such as gases. The analysis is essentially the same in both cases; however, more complex waves are possible in compressible fluids. Thus we must exercise care to ensure that only Alfvén waves are driven by a particular excitation in a compressible fluid.

12.2.4 Ferrohydrodynamics

Attention has been confined so far in this section to coupling with fluids that carry free currents. As pointed out in Section 8.5.2, magnetization forces can also be the basis for interaction with liquids. Commonly found fluids have no appreciable permeability. Ferromagnetic fluids, however, can be synthesized by introducing a colloidal suspension of magnetizable particles into a carrier fluid. Colloidal suspensions tend to settle out over long periods of time, and in the presence of a magnetic field the magnetized particles tend

* For an example of the experimental conditions necessary see A. Jameson, "A Demonstration of Alfvén Waves, I: Generation of Standing Waves," *J. Fluid Mech.*, **19**, 513–527 (August 1964).

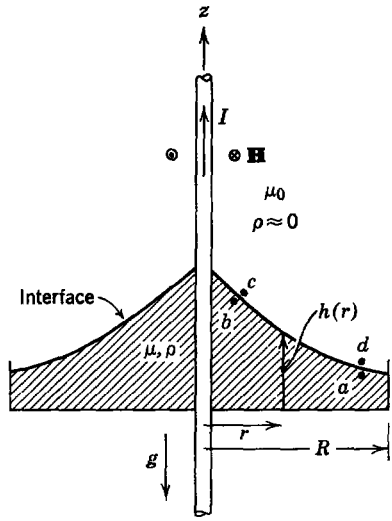

Fig. 12.2.21 A dish of magnetizable fluid is subjected to the magnetic field induced by current I.

to flocculate. Recent research efforts have led to the synthesis of colloidal suspensions (e.g., submicron-sized ferrite particles in a carrier fluid of kerosene), which are stable over indefinite periods of time.* We have no intention of delving into this topic in depth here; rather we confine ourselves to one simple example that illustrates this class of phenomena.

Although the ferrofluid is easily magnetizable, it can be made to be highly insulating against electrical conduction. In a magnetic field system the electric field is important because it determines the conduction current (through Ohm's law). In the region occupied by a magnetic insulator the conduction current is negligible and the equations for the magnetic field are simply

$$\nabla \times \mathbf{H} = 0, \tag{12.2.126}$$

$$\nabla \cdot \mathbf{B} = 0. \tag{12.2.127}$$

These are the equations used to describe the magnetic field, even in a dynamic situation. At any instant in time the magnetic field, at least insofar as it is determined by the magnetized fluid, has the same distribution as if the system were static.

As an illustration of the nature of the magnetization force consider the experiment shown in Fig. 12.2.21. A constant current I is imposed along the z-axis by means of a conductor. This conductor passes vertically through

* R. E. Rosensweig, "Magnetic Fluids," *International Sci. Technol.* **55**, 48–66, 90 (July 1966).

a dish containing the magnetic fluid. We wish to compute the static equilibrium of the fluid that results after the current I has been turned on. This amounts to determining the altitude h of the fluid interface above the bottom of the dish. We can expect that, because a force density, $-\mathbf{H}\cdot\mathbf{H}\nabla\mu$, tends to pull the fluid upward, the depth will be greatest where the magnetic field intensity is greatest.

We assume that the magnetic field induced by the return current can be ignored. Then, under the assumption of axial symmetry, Ampère's law requires that the current I induce an azimuthally directed magnetic field intensity

$$\mathbf{H} = \mathbf{i}_\theta \frac{I}{2\pi r}. \tag{12.2.128}$$

This problem is relatively simple because the magnetizable fluid has no effect on the distribution of $\mathbf{H}$; that is, because the physical system is axially symmetric, we can argue that the fluid deformations are also axially symmetric and $h = h(r)$. It is clear that (12.2.128) satisfies the field equations (12.2.126) and (12.2.127) in the region occupied by the fluid, and because the interface is axisymmetric it also satisfies the boundary conditions. The tangential component of $\mathbf{H}$ is continuous and there is no normal component of $\mathbf{B}$ at the liquid interface. Hence we know the magnetic field intensity at the outset, and this makes finding $h(r)$ straightforward.

The magnetic force acting on the fluid (from Section 8.5.2)* is

$$\mathbf{F} = -\tfrac{1}{2}\mathbf{H}\cdot\mathbf{H}\nabla\mu + \nabla\left(\tfrac{1}{2}\rho\frac{\partial\mu}{\partial\rho}\mathbf{H}\cdot\mathbf{H}\right). \tag{12.2.129}$$

In the bulk of the liquid, μ is constant. Hence the force density can be written as

$$\mathbf{F} = -\nabla\psi, \qquad \psi = -\frac{\rho}{2}\frac{\partial\mu}{\partial\rho}\mathbf{H}\cdot\mathbf{H}. \tag{12.2.130}$$

This is the form assumed in deriving Bernoulli's equation (12.2.11) which, in the case of a static fluid, becomes

$$p + \rho g z - \frac{\rho}{2}\frac{\partial\mu}{\partial\rho}\mathbf{H}\cdot\mathbf{H} = \text{constant}. \tag{12.2.131}$$

Remember that this equation is valid in the bulk of the fluid. It can therefore be used to relate the pressures and heights at the points (a) and (b) in Fig. 12.2.21. These points are just beneath the interface, where pressures are p_a and p_b, respectively, and the altitudes are h_a and h_b. From (12.2.131)

$$p_a + \rho g h_a - \frac{\rho}{2}\frac{\partial\mu}{\partial\rho}(H^a)^2 = p_b + \rho g h_b - \frac{\rho}{2}\frac{\partial\mu}{\partial\rho}(H^b)^2. \tag{12.2.132}$$

* See Table 8.1, Appendix G.

Similar reasoning shows that the pressures p_c and p_a just across the interface from points (b) and (a), respectively, are related by

$$p_c = p_a. \tag{12.2.133}$$

Here we have assumed that the density of the air above the liquid can be ignored.

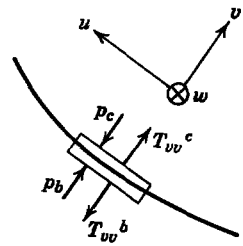

Fig. 12.2.22 A small volume element encloses the interface between points c and b in Fig. 12.2.21.

Now, if we could relate the pressures at adjacent points on opposite sides of the interface, we would have four equations that would make it possible to relate all four of the pressures p_a, p_b, p_c, and p_d. At the interface there is a jump in μ, and we must be careful to include the effect of the first term in (12.2.129) [which was not accounted for in (12.2.131)]. The stress tensor representation of the force density is convenient for determining the jump in pressure at the interface [see (8.5.41)].* A thin volume is shown in Fig. 12.2.22, as it encloses the region of interface between points b and c. To make use of the stress tensor in cartesian coordinates we erect a set of orthogonal coordinates (u, v, w) at the interface, with w in the θ-direction. Force equilibrium then requires that the sum of the surface forces balance

$$p_b - p_c = T_{vv}{}^b - T_{vv}{}^c = \tfrac{1}{2}(H^b)^2\left[\mu_0 - \mu\left(1 - \frac{\rho}{\mu}\frac{\partial\mu}{\partial\rho}\right)\right]. \tag{12.2.134}$$

Similarly, at the interface between points (d) and (a)

$$p_d - p_a = -\tfrac{1}{2}(H^a)^2\left[\mu_0 - \mu\left(1 - \frac{\rho}{\mu}\frac{\partial\mu}{\partial\rho}\right)\right]. \tag{12.2.135}$$

Now addition of these last four equations eliminates the pressures and gives an expression for the difference in surface elevation at points a and b as a function of the magnetic field intensities.

$$\rho g(h_a - h_b) = \tfrac{1}{2}(\mu_0 - \mu)[(H^b)^2 - (H^a)^2]. \tag{12.2.136}$$

Until now we have not specified the field intensity at points a and b. It has been known all along, however, because of (12.2.128). In particular, if we take the point a as being at $r = R$ (which could be the outside radius of the pan), (12.2.136) becomes an expression for the dependence of interface altitude on the radius r.

$$\rho g(h_b - h_a) = \tfrac{1}{2}(\mu - \mu_0)\frac{I^2}{(2\pi)^2}\left(\frac{1}{r^2} - \frac{1}{R^2}\right). \tag{12.2.137}$$

This result is sketched in Fig. 12.2.23. We have assumed that the density of the liquid is constant. This means that the total volume of the liquid must be

* Table 8.1, Appendix G.

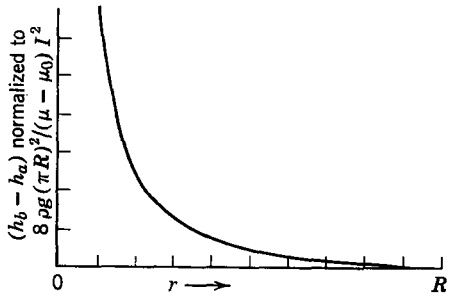

Fig. 12.2.23 Sketch of the liquid interface contour predicted by (12.2.137).

conserved, a fact that could be used to find the distance from a to the bottom of the pan.

An experiment with essentially the same ingredients as this example is shown in Fig. 12.2.24. In actuality, a significant magnetic saturation of the liquid makes the electrically linear model used here ($\mathbf{B} = \mu\mathbf{H}$) only approximately correct. As we know from Chapters 3 and 8, energy methods can also be used to calculate magnetization forces for electrically nonlinear systems, and this is what is required to make a careful comparison of theory and experiment.

Finally, it is worthwhile to observe that the magnetostriction force density has no observable effect on the surface deformation. This will always be the case as long as interest is confined to situations in which the fluid density remains essentially constant.

12.3 ELECTRIC FIELD COUPLING WITH INCOMPRESSIBLE FLUIDS

There is a wide range of mechanisms by which an electric field can produce a force on a fluid. In this section examples are used to illustrate two of the most commonly encountered types of interaction.

12.3.1 Ion-Drag Phenomena

Electrical forces can be produced in highly insulating gases and liquids by injecting charged particles and using an electric field to pull them through the fluid. Here we assume that these charged particles are ions that might be emitted by the corona discharge in the neighborhood of sharply pointed electrodes placed at a high potential (several kilovolts). These ions move through a liquid or gas under the influence of an applied electric field. Their motion, however, is retarded by friction, and momentum is imparted to the fluid. Therefore the ion-drag effect can be used to pump or accelerate the fluid. Similarly, if the ion is transported by the fluid against the retarding

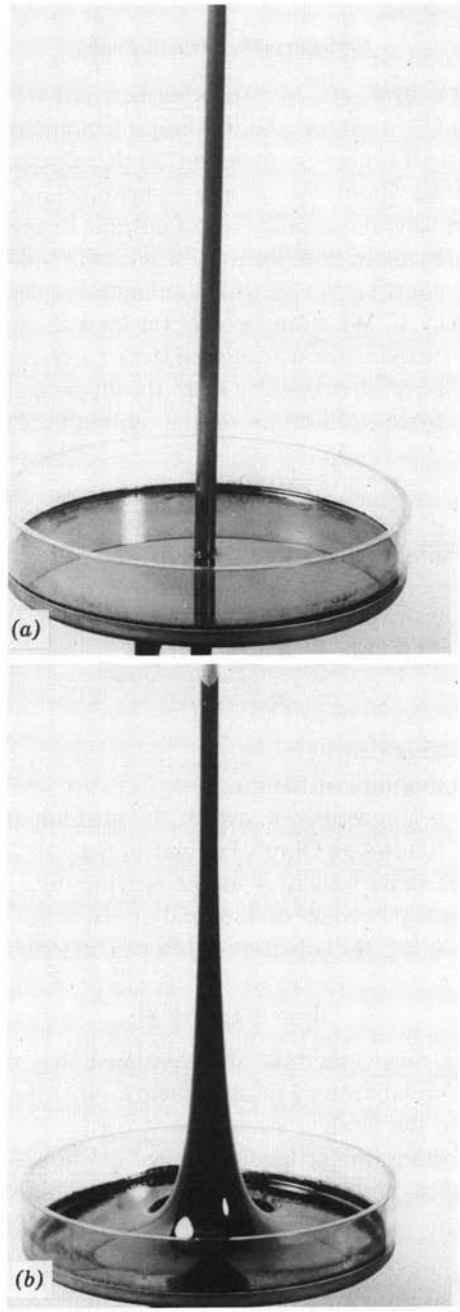

Fig. 12.2.24 (*a*) A conductor passes along the axis of symmetry through a pan containing the magnetizable liquid, $I = 0$. (*b*) The current I has been turned on. The result is a force density $-\mathbf{H} \cdot \mathbf{H}\nabla\mu$ that tends to lift the fluid upward, as predicted by (12.2.137). (Courtesy of AVCO Corporation, Space Systems Division.)

force of the electric field, energy can be transferred from the flow into an electrical circuit. In this context the ion-drag phenomenon is the basis for a gaseous Van de Graaff generator analogous to that discussed in Section 7.2.2.

To be quantitative about the ion-drag phenomenon we require a constitutive law to describe the conduction of current through the fluid. Here a simple picture of the force equilibrium for a single ion is helpful. Suppose that an ion with a charge q moves with a velocity $\mathbf{v}_r$ relative to the gas in an electric field intensity $\mathbf{E}$. We would expect (at least at atmospheric pressure) that the ion would experience a frictional drag force proportional (say, by the constant γ) to the relative velocity $\mathbf{v}_r$. In the absence of appreciable effects from acceleration, force equilibrium on the ion requires that

$$\mathbf{v}_r = \frac{q\mathbf{E}}{\gamma}. \tag{12.3.1}$$

If we let n be the number density of the ions, then the current density is

$$\mathbf{J}_f = nq\mathbf{v}_r, \tag{12.3.2}$$

which, in view of (12.3.1), can also be written

$$\mathbf{J}_f = \rho_f \mu \mathbf{E}, \tag{12.3.3}$$

where ρ_f = free charge density $= nq$,
$\mu = q/\gamma$ = mobility of the ion.

Equation 12.3.3 is a constitutive law for the medium at rest and plays the same role in what follows as Ohm's law did in Section 7.2. This law holds in a frame with the same velocity $\mathbf{v}$ as the moving fluid, where it would be written as $\mathbf{J}_f' = \rho_f \mu \mathbf{E}'$. In view of the field transformations for an electric field system (Table 6.1)*, the constitutive law can be written in the laboratory frame as

$$\mathbf{J}_f = \rho_f(\mu\mathbf{E} + \mathbf{v}). \tag{12.3.4}$$

In the example we now undertake it is assumed that the mobility μ is a constant, found from laboratory measurements. Note that $\mu\mathbf{E}$ is the velocity of an ion relative to the fluid.

An electrostatic pump might be constructed as shown in Fig. 12.3.1. The system consists of a nonpolarizable ($\epsilon = \epsilon_0$) gas flowing with constant velocity

$$\mathbf{v} = \mathbf{i}_z v_o \tag{12.3.5}$$

through a cylindrical insulating tube of cross-sectional area A. At $z = 0$ and $z = l$, plane conducting screens are placed perpendicular to the axis. We assume that the screens do not affect the gas flow but make electrical contact with the gas. The screens are connected to external terminals that are excited

* Appendix G.

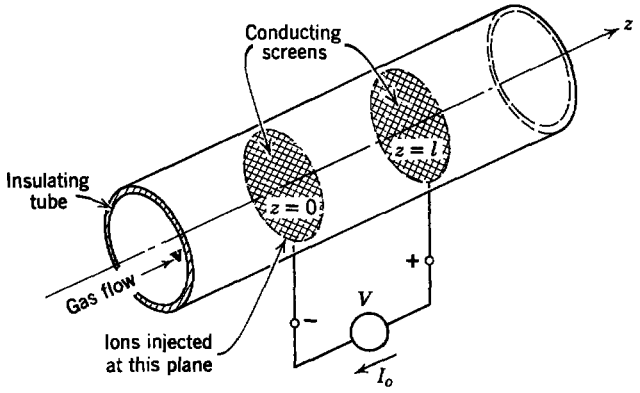

Fig. 12.3.1 Configuration for a gaseous electrostatic pump or generator.

by the constant-current source I_o as shown. At the plane $z = 0$ positive ions are injected into the gas by a source of ions.

For now we assume that this source supplies ions at a rate necessary to maintain the charge density ρ_o at the inlet screen:

$$\text{at } z = 0, \qquad \rho_f = \rho_o. \tag{12.3.6}$$

The current density and electric field intensity are assumed to have only z-components,

$$\begin{aligned} \mathbf{J}_f &= \mathbf{i}_z J, \\ \mathbf{E} &= \mathbf{i}_z E, \end{aligned} \tag{12.3.7}$$

and to be functions of z alone. Attention is confined to steady-state operation.

In addition to the boundary condition of (12.3.6), the equations we need to solve this problem are the z-component of (12.3.4)

$$J = \rho_f(\mu E + v_o), \tag{12.3.8}$$

Gauss's law written as

$$\epsilon_0 \frac{dE}{dz} = \rho_f, \tag{12.3.9}$$

and the conservation of charge for steady-state conditions

$$\frac{dJ}{dz} = 0. \tag{12.3.10}$$

The area over which current flows is A; consequently, the current density and the source current are related by

$$J = \frac{I_o}{A}. \tag{12.3.11}$$

We first solve (12.3.8) for the electric field intensity to obtain

$$E = -\frac{v_o}{\mu} + \frac{J}{\rho_f \mu}. \tag{12.3.12}$$

Next, this expression is differentiated with respect to z and (12.3.9) is used to eliminate E:

$$\frac{\rho_f}{\epsilon_0} = \frac{d}{dz}\left(\frac{J}{\rho_f \mu}\right). \tag{12.3.13}$$

Expansion of the derivative and use of (12.3.10) yields

$$\frac{d\rho_f}{dz} = -\frac{\mu}{\epsilon_0 J}\rho_f^3. \tag{12.3.14}$$

Integration of this expression, use of the boundary condition of (12.3.6), and some manipulation yield

$$\frac{\rho_f}{\rho_o} = \left[1 + \frac{2}{\mathrm{R}_e}\left(\frac{\rho_o v_o}{J}\right)\frac{z}{l}\right]^{-1/2}, \tag{12.3.15}$$

where $\mathrm{R}_e = \epsilon_0 v_o / \rho_o \mu l$ is the electric Reynolds number.

The plot of the free charge density shown in Fig. 12.3.2 makes it evident that the rate of decay down the channel is decreased as the electric Reynolds number is increased.

Substitution of (12.3.15) into (12.3.12) gives the electric field intensity between the grids

$$E = \frac{v_o}{\mu}\left\{-1 + \frac{J}{\rho_o v_o}\left[1 + \frac{2}{\mathrm{R}_e}\left(\frac{\rho_o v_o}{J}\right)\left(\frac{z}{l}\right)\right]^{1/2}\right\}. \tag{12.3.16}$$

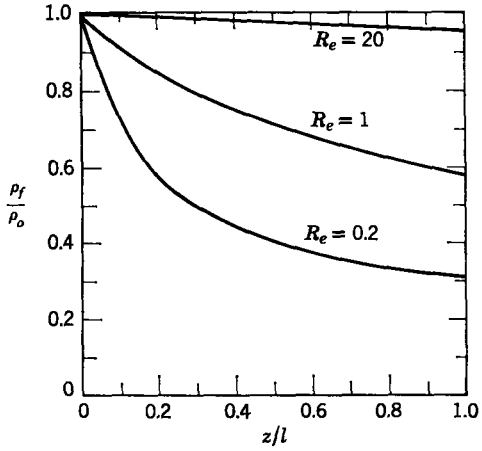

Fig. 12.3.2 Charge-density distribution between grids. $J/\rho_o v_o = 1$.

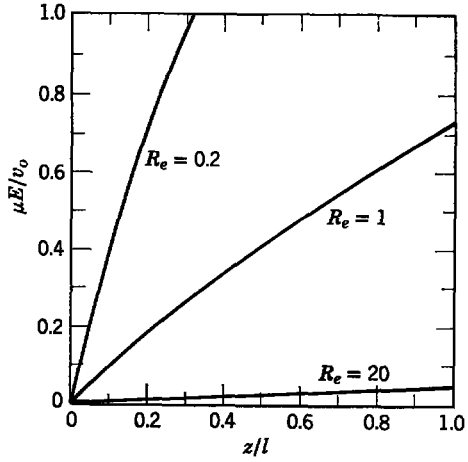

Fig. 12.3.3 Distribution of electric field intensity between the grids. $J/\rho_o v_o = 1$.

If the ion source at $z = 0$ is essentially limited by space charge, it will emit just enough charge to make the electric field at $z = 0$ vanish.* From (12.3.16) this requires that

$$\frac{J}{\rho_o v_o} = 1. \tag{12.3.17}$$

In our discussion it is assumed that J, ρ_o, and v_o are positive. Remember that μE is the velocity of the ions relative to the fluid. This condition requires that the ions have the same velocity as the fluid at $z = 0$. Then the electric field is positive everywhere between the grids, as shown in Fig. 12.3.3. This means that the ions move more rapidly than the fluid and, as we shall see, the system operates as a pump.

As for the MHD machine discussed in Section 12.2.1, two "terminal" characteristics of the electrohydrodynamic flow interaction are of interest—the pressure change from inlet to outlet and the terminal voltage. The first can be computed from the electric field intensity by making use of the Maxwell stress tensor†. The pressure forces acting on the fluid in the channel section between $z = 0$ and $z = l$ are just balanced by the Maxwell stresses acting over the surface enclosing this section. Because there are no electrical shear forces,

$$A[p(l) - p(0)] = A[T_{11}(l) - T_{11}(0)] = \tfrac{1}{2} A\epsilon_0[E^2(l) - E^2(0)]. \tag{12.3.18}$$

Since we have constrained $E(0)$ to vanish, it is clear from this statement that

* For a discussion of this model for the ion source see O. M. Stuetzer, "Ion Drag Pumps," *J. Appl. Phys.*, **31**, 136 (January 1960).

† Section 8.3 or Appendix G.

$p(l) > p(0)$. In fact, from (12.3.16)

$$p(l) - p(0) = \frac{\epsilon_0}{2}\left(\frac{v_o}{\mu}\right)^2\left[-1 + \left(1 + \frac{2}{R_e}\right)^{1/2}\right]^2. \tag{12.3.19}$$

This result indicates that the larger R_e, the smaller the pressure rise between the grids. This is misleading because both the electric Reynolds number R_e and the first factor in (12.3.19) depend on v_o. If we think of holding v_o fixed, however, and recall that R_e is inversely proportional to l, (12.3.19) shows that the pressure rise increases as l increases.

To obtain the terminal voltage V we integrate the negative of the electric field intensity from $z = 0$ to $z = l$:

$$V = \frac{lv_o}{\mu}\left\{1 - \frac{R_e}{3}\left[\left(1 + \frac{2}{R_e}\right)^{3/2} - 1\right]\right\}. \tag{12.3.20}$$

This voltage is negative, as must be the case if power is supplied by the current source to the fluid. The fact that there is a pressure rise in the direction of flow indicates that work is done on the fluid as it passes through the region between the grids.

Ion-drag interactions can be used not only to pump slightly conducting fluids but also for conversion of energy from mechanical to electrical form.* In gases the mobility of ions is so great that such devices tend to lack efficiency. This shortcoming can be obviated either by using liquids, in which the mobility of ions tends to be much lower, or by replacing the ions with larger charged particles of liquid or solid. In any case, the electric pressure $\frac{1}{2}\epsilon_0 E^2$ tends to be small compared with the magnetic pressure $\frac{1}{2}\mu_0 H^2$ because the electric field intensity is limited by the breakdown strength of the dielectric medium. Hence *for a given size of device* the amount of energy converted in an electric field interaction is much less than that found for a magnetic field interaction.

One of the most significant reasons for our discussion of the ion-drag phenomenon is that it is commonly (and altogether too easily) encountered in high voltage systems, in which it accompanies corona discharge. A simple laboratory demonstration of the effect is shown in Fig. 12.3.4, in which two wire grids are placed at a potential difference of about 25 kV. Perpendicular segments of wire are mounted on the lower electrode to form a "bed of nails," and when this grid is electrified the tips of these segments provide sites for corona discharge. This discharge is the source of ions at $z = 0$ in Fig. 12.3.1.

* B. Kahn and M. C. Gourdine, "Electrogasdynamic Power Generation," *AIAA J.*, **2**, No. 8, 1423–1427 (August 1964). Also, A. Marks, E. Barreto, and C. K. Chu, "Charged Aerosol Energy Converter," *AIAA J.*, **2**, No. 1, 45–51 (January 1964).

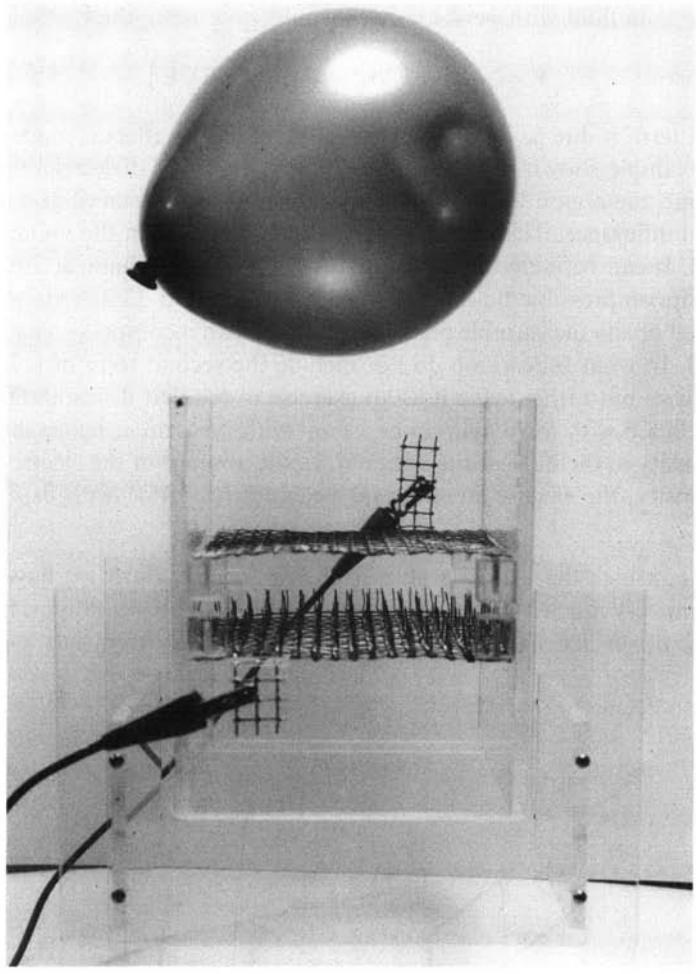

Fig. 12.3.4 Simple laboratory demonstration of ion-drag effect. In the absence of an applied voltage the balloon rests on the plastic enclosure. With voltage, it is pushed upward by ions being conducted between the grids.

In the absence of an applied voltage, the balloon rests on the plastic enclosure. With voltage, it is pushed upward by the pumping action between the grids.

12.3.2 Polarization Interactions

The analog to the magnetization interactions with fluids, discussed in Section 12.2.4, is the polarization interaction with electric fields—sometimes referred to as "dielectrophoresis." The polarization force density for fluids was developed in Section 8.5, in which it was found that in the absence of

free charges a fluid with permittivity ϵ would experience the force density*

$$\mathbf{F} = -\tfrac{1}{2}\mathbf{E}\cdot\mathbf{E}\nabla\epsilon + \nabla\left(\tfrac{1}{2}\rho\frac{\partial\epsilon}{\partial\rho}\mathbf{E}\cdot\mathbf{E}\right). \tag{12.3.21}$$

The first term is due to inhomogeneity of the fluid. Its effect is made familiar by the example shown in Fig. 8.5.6, in which a slab of dielectric material is pulled into the region between plane-parallel electrodes placed at a constant potential difference. The second term is due to changes in the volume of the material. It can be included in the analysis of electromechanical interactions with an incompressible fluid, but as we saw in Section 12.2.4, its effect will cancel out of any measurable prediction based on an incompressible model for the fluid. In what follows we do not include the second term of (12.3.21) in our analysis but rather leave it as an exercise to see that it has no effect. We are concerned with the dynamics of a fluid with uniform ϵ; hence there is no force density in the bulk of the material. In the absence of the electrostriction force density, the electric stress tensor becomes [(8.5.46)* with $\partial\epsilon/\partial\rho = 0$]

$$T_{ij} = \epsilon E_i E_j - \tfrac{1}{2}\delta_{ij}\epsilon E_k E_k. \tag{12.3.22}$$

Now consider the example shown in Fig. 12.3.5. Here we have a fluid pendulum very much like that shown in Fig. 12.2.7. This pendulum, however, is upside down because g is directed upward. The problem has a practical

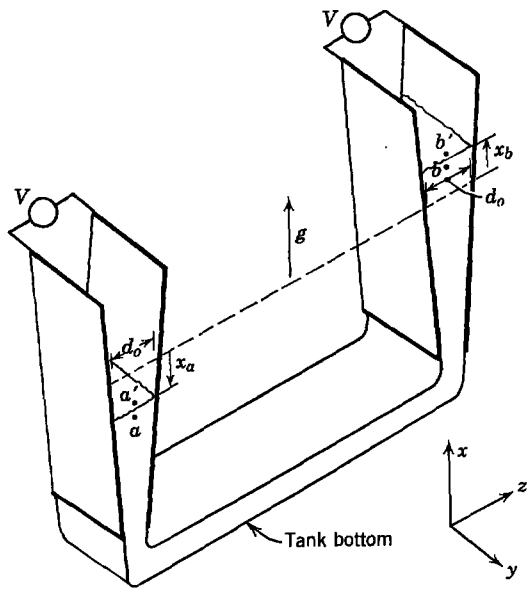

Fig. 12.3.5 A liquid pendulum containing dielectric fluid. Slightly diverging plates are used to impose a spatially varying electric field that tends to maintain the liquid in the bottom of the tank in spite of the acceleration g.

* See Table 8.1, Appendix G.

basis. Suppose that we wish to use the electric field to provide an artificial "gravity" to bottom the fluid within a tank under the near-zero gravity conditions of outer space; for example, the fluid might be the cryogenic liquid fuel used to propel a spacecraft. The electric field then provides fluid at a drain placed at the "bottom" of the tank. In this case g represents the effect of acceleration of the vehicle, as, for example, that which would occur during attitude control maneuvers. We have chosen g to be upward because this appears to be the worst possible situation in terms of removing the fluid from the bottom of the tank.

The U-shaped tank is considered in this example because it is easily analyzed with the tools developed in this chapter. Even though the example may seem academic, it has practical significance in the design of fluid orientation systems.

Because there are no electrical forces in the bulk of the liquid, we can use Bernoulli's equation derived in Section 12.2.1*b*. Again we carry out an integration of the momentum equation, as indicated by (12.2.33*a*), between points a and b, defined in Fig. 12.3.5. Now, however, the interfaces are subject to surface forces [due to the first term in (12.3.21)], and we cannot claim that the pressures p_a and p_b (just below the respective interfaces) are equal. In carrying out the integral of (12.2.33*a*) we retain the pressures evaluated at the points a and b to obtain

$$\rho l \frac{\partial v}{\partial t} = 2\rho g x_a + p_a - p_b. \tag{12.3.23}$$

Here v is the velocity of the fluid directed from a to b so that

$$\frac{\partial v}{\partial t} = \frac{d^2 x_a}{dt^2}. \tag{12.3.24}$$

We have approximated the velocity as being the same along a streamline connecting the points a and b. The cross-sectional area of the pendulum varies somewhat because the vertical legs are constructed with side walls composed of slightly diverging electrodes. Insofar as the fluid velocity is concerned, the effect of the diverging plates represents a nonlinear effect equivalent to slight changes in the length l of the pendulum; this effect is ignored here.

The fundamental difficulty in keeping the liquid in the bottom of the tank, with no electric field, is illustrated by combining the last two equations. With no applied voltage, $p_a = p_b$, and it is clear that the equilibrium represented by $x_a = 0$ is unstable. It is the purpose of the electric field to stabilize this equilibrium.

Before completing the mathematical representation of the dynamics consider physically how the polarization force density [the first term in

(12.3.21)] can stabilize the equilibrium at $x_a = 0$. This force is finite only at the two interfaces, where it is singular (infinite in magnitude over an infinitely thin region of space); that is, it comprises a surface force directed in the positive x-direction on each of the interfaces in proportion to the square of the electric field intensity. With the pendulum in equilibrium, the electrical forces on each of the interfaces just balance. Suppose that the system is perturbed to the position shown in Fig. 12.3.5. Then the upward-directed force on the interface at a is increased (the plates are closer together at this point; therefore $\mathbf{E}$ is greater), whereas that at b is decreased. This tends to return the pendulum to its equilibrium position. We expect that if we can make this stabilizing electrical effect large enough it will outweigh the de-stabilizing effect of gravity.

To provide a quantitative statement of the condition for stability we complete the equation of motion by relating the pressures p_a and p_b. Force balance on the interfaces, in view of the force diagrams shown in Fig. 12.3.6, requires

$$p_{a'} - p_a = T_{11}{}^{a'} - T_{11}{}^{a} = -\tfrac{1}{2}(\epsilon_0 - \epsilon)\left(\frac{V}{d_a}\right)^2, \tag{12.3.25}$$

$$p_{b'} - p_b = T_{11}{}^{b'} - T_{11}{}^{b} = -\tfrac{1}{2}(\epsilon_0 - \epsilon)\left(\frac{V}{d_b}\right)^2. \tag{12.3.26}$$

Of course, the spacing d used in these expressions is evaluated at the instantaneous locations of the respective interfaces.

$$d_a = d_o - cx_a, \tag{12.3.27}$$

$$d_b = d_o + cx_b. \tag{12.3.28}$$

Here c is determined by the rate at which the electrodes diverge. Then, to linear terms, the combination of (12.3.25) and (12.3.26) (remember, $x_a = x_b$) gives

$$p_a - p_b + p_{b'} - p_{a'} = -2c(\epsilon - \epsilon_0)\left(\frac{V}{d_o}\right)^2\left(\frac{x_a}{d_o}\right). \tag{12.3.29}$$

Formally, we can see that $p_{b'} = p_{a'}$ by joining points a' and b' with a streamline passing through the fluid above the interfaces (where the vapor phase is present and density is negligible). Then, by combining (12.3.25), (12.3.26),

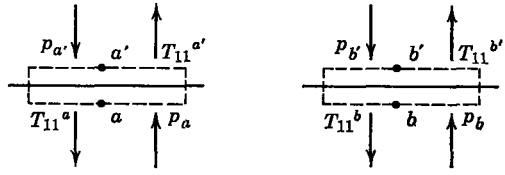

Fig. 12.3.6 Force equilibrium for each of the interfaces shown in Fig. 12.3.5.

and this last expression, we obtain the required equation of motion for the pendulum:

$$\rho l \frac{d^2 x_a}{dt^2} + x_a\left[-2\rho g + 2c(\epsilon - \epsilon_0)\frac{V^2}{d_o^3}\right] = 0. \tag{12.3.30}$$

From this it is clear that the equilibrium is stable if the voltage is made large enough to satisfy the condition

$$c(\epsilon - \epsilon_0)\frac{V^2}{d_o^3} > \rho g. \tag{12.3.31}$$

Liquid being oriented under near-zero gravity conditions is shown in Fig. 12.3.7. Each pair of adjacent plates has a potential difference. The zero gravity situation was created by flying the experiment within a KC-135 in a near-zero gravity trajectory. The liquid is Freon 113 with aniline dye added for purposes of observation. The basic mechanism for orienting the liquid is the same as that for the example considered in this section. Any two pairs of diverging plates can be considered as constituting a fluid pendulum with the essential behavior of that shown in Fig. 12.3.5. The stability condition of (12.3.31) guarantees that the equilibrium with the fluid in the tank "bottom" will be stable. Of course, a more complete representation of the dynamics requires a continuum model,* for instability may develop in the region between a single pair of electrodes.

We have stated from the outset that free charge forces are of negligible importance. In practice, this is guaranteed by making the applied voltages V of alternating polarity with sufficiently high frequency that free charges cannot relax into the fluid. If the frequency is high compared with typical mechanical frequencies, it is possible to use the same mathematical model as that developed here, except that V is the rms value of the voltage.

12.4 DISCUSSION

In this chapter we have introduced some of the fundamental laws and analytical techniques that are used in the study of electromechanical interactions with conducting, magnetizable and polarizable fluids. We have applied these laws and techniques to the analysis of systems in which an incompressible, inviscid fluid model is appropriate. Even though the incompressible, inviscid fluid model may seem quite restrictive, it provides an understanding of the basic electromechanical interactions that occur in all sorts of magnetohydrodynamic and electrohydrodynamic systems, including those with gaseous conductors.

* In fact, a description of this mode of instability is given in Section 10.1.

Fig. 12.3.7 Orientation system for storing liquids within a tank in the zero gravity environment of space. The tank used in this test was spherical and transparent, with circular electrodes which are seen here edge-on. The electrodes converge toward the bottom of the picture; thus this is the region in which the electric field should provide an artificial "bottom." (*a*) With one g acting toward the *top* of the picture and no electric field, the liquid is in the upper half of tank; (*b*) liquid oriented at artificial "bottom" of tank under near-zero-gravity conditions created by flying the tank within a KC-135 in a zero gravity trajectory. The electrodes are at alternate polarities and can be viewed as a combination of pendulums with the basic configuration shown in Fig. 12.3.5. (Courtesy of Dynatech Corp., Cambridge, Mass.)

In Chapter 13 the restriction of an incompressible fluid is relaxed, and the effects of compressibility on electromechanical interactions are studied, although the restriction to inviscid fluid models is still retained.